Aus der Neurologischen Klinik und Poliklinik mit Friedrich-Baur-Institut
der Ludwig-Maximilians-Universität München
Direktorin: Univ.-Prof. Dr. med. Marianne Dieterich, FANA, FEAN

Laser capture microdissection of single muscle fibers for mitochondrial proteomic investigations

Dissertation
zum Erwerb des Doktorgrades der Medizin
an der Medizinischen Fakultät der
Ludwig-Maximilians-Universität zu München

vorgelegt von
Jing Tan
aus
Shandong (China)

2019

Mit Genehmigung der Medizinischen Fakultät

der Universität München

Berichterstatter:	Prof. Dr. med. Thomas Klopstock
Mitberichterstatter:	Prof. Dr. Dejana Mokranjac
	Prof. Dr. Marcus Deschauer
Mitbetreuung durch die promovierte Mitarbeiterin:	Dr. Marta Murgia
Dekan:	Prof. Dr. med. dent. Reinhard Hickel
Tag der mündlichen Prüfung:	21.02.2019

Table of Contents

List of tables

List of figures

Introductory note

Major parts of this work are included in the yet unpublished (as of Sept 2018) manuscript

Title: **Single muscle fiber proteomics in mitochondrial disorders highlights fiber type-specific adaptations to respiratory chain defects**

Authors: Marta Murgia, Jing Tan, Philipp E. Geyer, Sophia Doll, Matthias Mann* and Thomas Klopstock*

1. Introduction

1.1 Mitochondria

Mitochondria are 0.5-1.0 micron organelles, first described by Richard Altmann in 1890. They are enclosed in a double membrane, the outer and inner membrane, separating the mitochondrial matrix from the surrounding cytoplasm. The outer mitochondrial membrane (OMM) is smooth and interspersed with voltage-dependent anion channels (VDAC), also called porins, which provide tunnels for the passage of small ions, metabolites and proteins (~5kDa) into the intermembrane space between the outer and inner membrane [1]. In comparison to the outer membrane, the inner mitochondrial membrane (IMM) is less permeable and highly invaginated, folding many times to create layered structures termed cristae, which increase the surface area of the membrane for various chemical reactions. The mitochondrial matrix lies within the inner membrane and contains a variety of enzymes and proteins responsible for the bioenergetic and biosynthetic pathways of ATP, mitochondrial ribosomes, tRNAs and mitochondrial DNA (mtDNA) [2].

1.1.1 Evolution of mitochondria

Mitochondria are the only organelles containing DNA independent of the nuclear-enclosed chromosomal DNA (nDNA) in animal cells. To better understand the mitochondrial genome and related proteins, the events resulting in the mitochondria becoming a relatively independent part of the eukaryotic cell need to be discussed.

The endosymbiotic theory, as a model for explaining mitochondrial origin, arose in the nineteenth century [3]. According to this theory, mitochondria evolved from free-living bacteria which were incorporated into eukaryotic host cells via the process of endocytosis [3, 4]. And indeed, it is strongly supported by gene sequence data that the monophyletic origin of mitochondria from a common eukaryotic ancestor, a subgroup of the α-Proteobacteria, emerged more than two billion years ago [5]. The proliferation of mitochondrial proteins is

therefore coordinated by the mitochondria's own cycle in a similar manner to bacterial division. However, due to redundancy, the majority of endosymbiotic genes of the mitochondria and plastids have been lost in the past two billion years. [6] As a consequence, while the nuclear genome has become diverse and more complex, the mitochondria have retained just a small number of genes in their genome. Accordingly, analysis of mitochondrial proteomes demonstrates that only 22% of human mitochondrial proteins are kept from protomitochondrial descent [6].

1.1.2 Mitochondria and oxidative phosphorylation (OXPHOS)

Mitochondria provide the essential biological energy to cells by continual generation of adenosine triphosphate (ATP) via respiratory chain oxidative phosphorylation (OXPHOS). The mitochondria are therefore referred to as the cellular energy factories. The mitochondrial respiratory chain, otherwise known as the electron transport chain (ETC), is comprised of five enzyme complexes residing in the IMM (**Figure 1.1**). The production of ATP requires a constant supply of mitochondrial respiratory substrates, adenosine diphosphate (ADP) and inorganic phosphate (Pi). The carrier family proteins of the mitochondria, such as ADP-ATP translocase, phosphate carrier protein and citrate transport protein, constantly work to ensure the smooth progress of cellular metabolic processes between the mitochondria and the cytoplasm [7, 8].

The mitochondrial respiratory chain generates a electrochemical proton gradient between the mitochondrial matrix and the intermembrane space by the transfer of electrons along the respiratory chain complexes, and the eventual transfer to molecular oxygen (O_2). In brief, the reduction equivalents (NADH and $FADH_2$) from glycolysis, the tricarboxylic acid (TCA) cycle and from β-oxidation, release their electrons for uptake by the respiratory chain [9]. The electron transfer of the respiratory chain is enabled by various prosthetic groups, such as iron-sulfur (Fe-S) clusters in complex I, II and III and by the heme group in cytochrome C and complex IV. In complex I (NADH dehydrogenase) electrons are delivered from the oxidation of NADH, in complex II (succinate dehydrogenase) from the oxidation of succinate via flavin

adenine dinucleotide (FAD), and additionally, electron transfer flavoprotein (ETF) transfers electrons originating from β-oxidation to the electron transport chain. After the electrons access the respiratory chain, the lipophilic molecule coenzyme Q (CoQ) is reduced from its ubiquinone form to ubiquinol. The electrons pass to complex III (cytochrome C reductase) which in turn transfers them to cytochrome C. The water-soluble protein cytochrome C shuttles electrons in the IMS between respiratory chain complexes III and IV, the cytochrome oxidase (COX). COX catalyzes the final reaction, the reduction of O_2 to water and thus generates the electrochemical gradient.

Through this transfer of electrons, the process of oxidative phosphorylation (OXPHOS) leads to the active pumping of hydrogen ions across the IMM to the intermembrane space, and the resulting electrochemical proton gradient drives the synthesis of ATP from ADP and inorganic phosphate (Pi) by complex V (ATP-synthase) [10]. The synthesized ATP can subsequently be used for all active metabolic processes.

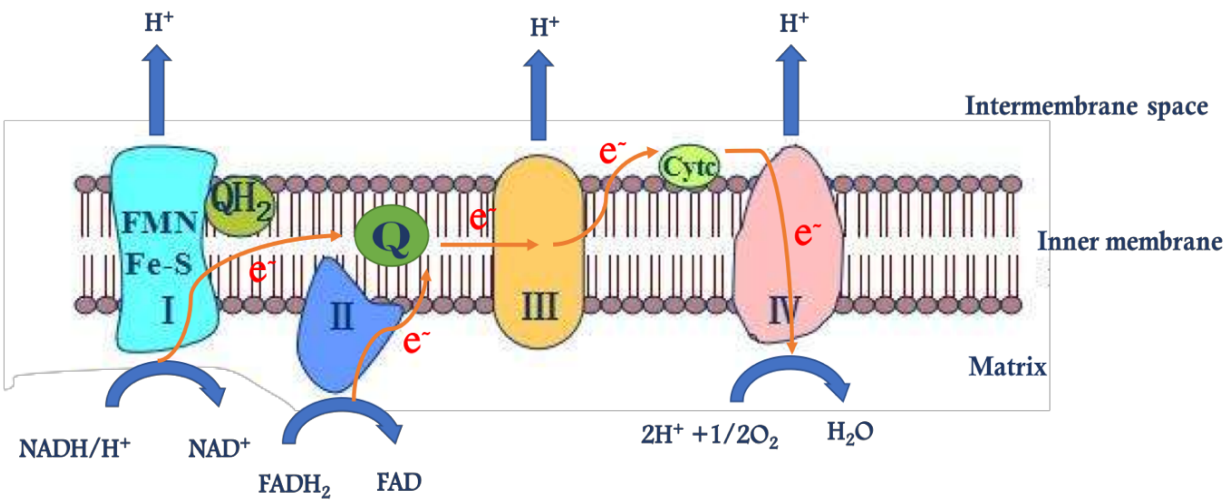

Figure 1.1: The electron transport chain (ETC). ETC shuttles electrons from NADH and FADH2 to O_2 (orange arrows) forming H_2O via four protein complexes (Complex I-IV) embedded in the inner mitochondrial membrane. In the process, protons (H^+ ions) are pumped from the mitochondrial matrix to the intermembrane space producing a proton gradient for subsequent ATP production by Complex V.

1.2 Human mitochondrial genome

Mitochondrion each contain their own small genome, the mitochondrial DNA (mtDNA). In 1963, Sylvan et al. firstly detected the DNA within mitochondria [11] and in 1981, Anderson et al. completed the sequence of the human mitochondrial genome [12]. The human mtDNA is a double-stranded circular, 16,569 bp molecule consisting of 37 genes which collectively encode 22 transfer RNAs (tRNA), 12S and 16S ribosomal RNAs (rRNA), and 13 core OXPHOS polypeptides. The numbers of mitochondria and mitochondrial genomes per cell is regulated and is distinct between different tissues [13]. Each mitochondrion typically contains 2–10 mtDNA copies [14], therefore 100–10,000 separate copies of mtDNA are generally estimated per somatic cell depending on the type and developmental stage of cell [14].

1.2.1 Structure of mtDNA

The structure and gene organization of mammalian mtDNA is highly conserved. It is a closed circular double-stranded DNA molecule made up of a H strand (heavy strand) and an L strand (light strand). The designations of the strands of the DNA duplex are derived from the different buoyant densities due to the asymmetric distribution of guanine and cytosine by the CsCl (cesium chloride) equilibrium gradient centrifugation [15]. The map of mammalian mtDNA is organized as shown in **Figure 1.2**. The origins of replication of the H and L strands are called as O_H and O_L respectively, and are significant landmarks of the ring-shaped mtDNA. The H strand runs with a 5'→3' polarity in a counter-clockwise direction, while the L stand runs with a clockwise polarity. The section from O_H to O_L in a clockwise direction is termed the large arc, the corresponding section from O_L to O_H is termed the small arc.

As opposed to nuclear DNA, mtDNA lacks an intron-exon structure. There are only two non-coding intergenic regions in mtDNA contributing a major component of the regulated expression unit. The major non-coding region is commonly known as the displacement loop (D-loop) spanning ~1 kb in humans and residing between the genes encoding $tRNA^{Phe}$ and $tRNA^{Pro}$, where it contains the O_H and the promoters for mtDNA transcription [16]. Here, the

two strands of the mtDNA are separated by a third strand. The D-loop is the most variable fragment of mtDNA due to high substitution. Given that the D-loop contains highly conserved elements with potential regulatory function, this variability increases the potential for deleterious mutations to arise [17, 18]. The second, shorter (30 nucleotide-long) non-protein coding region, is located around two-thirds of the mtDNA distance from the O_H and resides within a tRNA cluster, containing O_L.

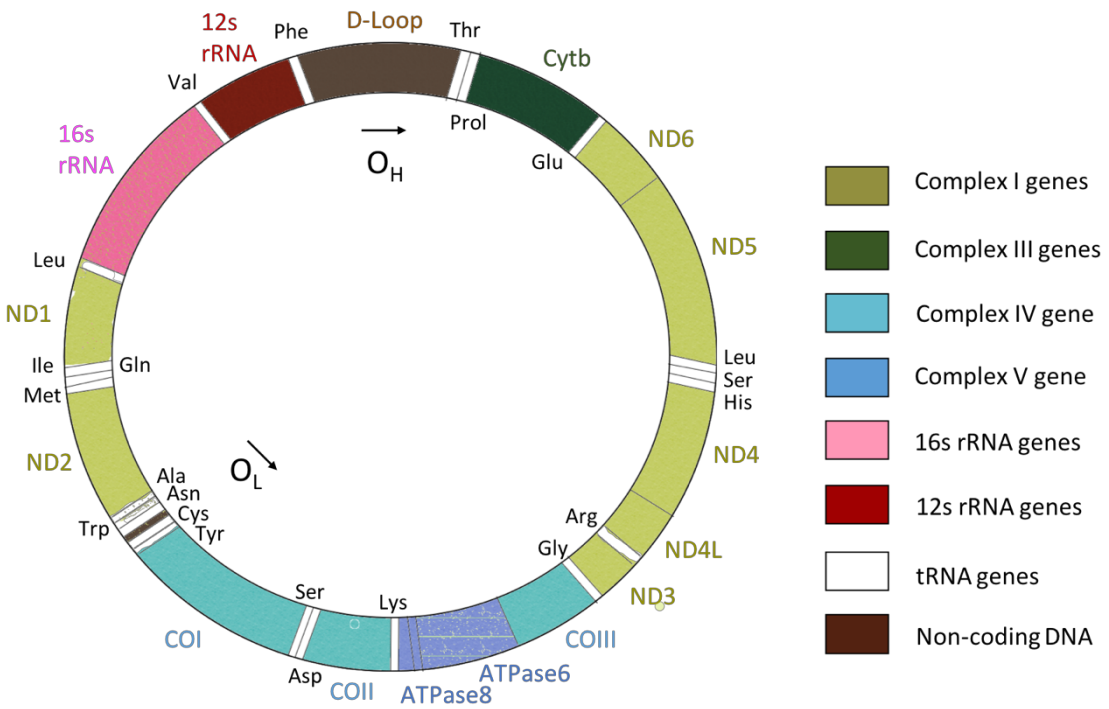

Figure 1.2: Structure of mitochondrial DNA. The respiratory chain complex genes, ribosomal RNA genes and non-coding DNA are colored respectively. The tRNA genes are designated by the abbreviation of the corresponding amino acid. The abbreviations of the protein-coding genes describe the encoded subunit of the respective respiratory chain complex.

1.2.2 Inheritance of mtDNA

It is generally considered that the human mtDNA is exclusively maternally inherited. However, a single case report of a patient with mitochondrial myopathy and inheritance of a pathogenic mtDNA mutation occurring on a paternal mtDNA background has been described

[19]. Furthermore, there are several lines of evidence for the rare paternal inheritance of mtDNA in other mammalian species [20].

1.2.3 Transcription products of mtDNA

It has been shown that both mtDNA strands are completely and symmetrically transcribed according to in vivo human and mouse cell models in mitochondrial studies. The majority of the protein-coding mtDNA genes are located on the H-strand, this includes two genes encoding rRNAs (12S and 16S rRNA), 14 genes encoding tRNAs and 12 protein-coding genes. Only a small amount of information is encoded on the L-strand, including genes for eight tRNAs and 1 protein-encoding gene (ND6).

Taking a closer look at the protein-coding genes (see **Figure 1.2**), the genes ND1, ND2, ND3, ND4, ND4L, ND5 and ND6 encode components of complex I. In mammals, complex I comprises 44 different subunits, seven encoded by mtDNA and 37 encoded by the nuclear DNA (nDNA) [21]. All four subunits of complex II are nuclear-encoded. In complex III, cytochrome b is the only mtDNA-encoded subunit, with the remaining 9 subunits encoded in the nDNA. Complex IV (cytochrome C oxidase) is a complex enzyme composed of 13 protein subunits. The larger active subunits, cytochrome oxidase (CO) I, II and III, are encoded by the mtDNA, with the remaining smaller subunits encoded by the nDNA [22]. Finally, the ATPase 6 and ATPase 8 genes, two of the 12 subunits of complex V (ATP synthase) are mtDNA-encoded and the remainder are nuclear-encoded. The mitochondrial genome therefore encodes rRNA and related tRNA molecules for their own intramitochondrial translation, in addition to the minority of the protein components of the respiratory complexes, with complex II entirely nDNA-encoded. In **Figure. 1.2**, the short genes for tRNAs can be seen to distribute throughout the entire circular mtDNA and are depicted in the figure with the respective amino acid-specific abbreviation. The two rRNA genes are found near the D-loop region in the counter-clockwise direction.

Mitochondrial protein synthesis therefore requires a plethora of different nuclear-encoded molecules, such as ribosomal proteins, ribosome assembly proteins and aminoacyl-tRNA synthetases (responsible for loading the mitochondrial tRNAs with amino acids) in addition to RNA polymerase and its transcription factors [23]. Accordingly, most mitochondrial translation proteins are encoded in the nucleus, synthesized in the cytosol, and imported into mitochondria, to assemble into functional respiratory complexes, allowing the generation of ATP through oxidative phosphorylation (OXPHOS).

1.2.4 Expression regulation of mtDNA

The principal function of the mitochondria is to generate the majority of the cellular energy in the form of ATP by OXPHOS. The expression of mtDNA is therefore the subject of tight regulation which requires the participation and coordination of two distinct genomes, the mitochondrial and nuclear genomes. However, the molecular mechanisms involved in expression regulation remain poorly understood. The expression of nuclear genes associated with mitochondrial function and protection is modulated by mitochondria-to-nucleus retrograde signaling mechanisms. These signaling pathways are controlled in part by mitochondrial metabolites, including Ca^{2+}, reactive oxygen species (ROS), and ATP [24]. Ca^{2+} is a ubiquitous intracellular signal mediating several cellular pathways, including Ca^{2+}-dependent PKC, CaMKII-CREB and JNK MAPK signaling pathways, and activation of calcineurin (CaN, an activator of NFATc and NF-κB), which are essential for muscle formation, growth and regeneration.

Furthermore, evidence shows that regulation of mtDNA expression can be achieved through adjusting the redox balance and ATP concentration. During recent decades, it has become clear that ROS serves as key signaling molecules in the regulation of biological and physiological processes. An extensive number of factors are defined as targets of ROS or sensitive to redox stress, such as cell-signaling proteins (NF-κB, MAPKs and PI3K-Akt), phospholipases A2 (PLA2), PLC and PlD, calcium channels, tyrosine phosphatases, and a number of protein kinases [24, 25], which play a key role as an antioxidant defense against

the intake of xenobiotics through the activation of antioxidant responsive elements (ARE). In terms of nDNA expression, the nuclear respiratory factor-1 (NRF-1) and NF2 regulate nuclear-encoded mitochondrial gene transcription and are necessary to maintain mitochondrial activity [26]. Both NRF-1 and NRF-2 can indirectly affect the nuclear transcription factor Yin-Yang 1 (YY1) leading to a reduction in the product of ATP/AMP ratio [27].

1.3 Mutations of mtDNA

The mutation rate of mtDNA is estimated to be more than 10 times higher than that of nDNA [28]. This results from multiple factors: Firstly, even in the presence of mtDNA repair systems, mitochondria are deficient in the ability to completely offset the persistent oxidative damage caused by ROS generated from the IMM which is in close proximity to the mitochondrial genome. And secondly, there is absence of protective histone molecules.

The first pathogenic mtDNA mutation in a human patient was reported in 1988 [29, 30]. Since then, over 300 disease-causing mtDNA mutations have been described, presenting with a wide variety of disease phenotypes.

The mutations of mtDNA, most often large deletion/duplication and point mutations, have their own unique characteristics. As the mitochondrial genome exists in many hundreds of copies in each eukaryotic cell, mutations may either affect all of the mitochondria (termed homoplasmy) or more commonly affect only a subset of the mitochondria (termed heteroplasmy). Thus, affected patient cells may contain a mixture of both wild-type mtDNA and mutated mtDNA, the distribution and proportion of which can vary widely between different organs and even between different cells of the same organ [31]. This uneven distribution of mutated mtDNA influences the physiological function of affected cells and contributes to a mosaic pattern of respiratory chain-deficiency cells in affected tissues. If a certain limit of mutational load is exceeded, leading to dysfunction of the respiratory chain, the patient will express the phenotype, termed the "threshold effect". The exact level of this

threshold is dependent upon the type and location of the mutation in the mitochondrial genome. For example, it has been reported that a 90% mutational load is required for some tRNA genes and ~60% for some deletion mutations to result in a clinical phenotype [32].

1.3.1 Classification of mtDNA mutations

Currently, due to the characteristics of mitochondrial inheritance and biogenesis, there is no single universal classification standard for mtDNA mutations. Correlation of clinical phenotype amongst mutation carriers is considered the most significant reference to estimate mtDNA mutation pathogenicity. The variant classification which is most commonly used is that presented by Wong J et al. 2012 (**Table 1.1**) [33]. In this classification, the publicly available MITOMAP (http://www.MITOMAP.org/MITOMAP) and the Human Mitochondrial Genome Database mtDB (http://www.mtdb.igp.uu.se/) databases are referred to.

The discovery of a novel rare mutation in the mtDNA allows the diagnosis of mitochondrial disease and subsequent genetic counselling. However, due to the relatively high mutation rate of mtDNA, it should be taken into consideration that any novel variant detected by complete mitochondrial genome sequencing requires further supporting evidence to determine its pathogenicity. For example, correlation in the specific clinical manifestation between mutation carriers and targeted sequencing of the patient's mother and other matrilineal relatives will benefit to make further function analyses of pathogenicity.

Table 1.1: Criteria for the classification of mtDNA variants by pathogenicity.

mtDNA mutation	Criteria
Pathogenic variant	mtDNA contains a variant that is listed in the MITOMAP database as a "confirmed mutation" and has been annotated in relation with several unrelated patients/families with clinical correlation and/or supporting functional evidence of pathogenicity
Unclassified variant	mtDNA variant meeting at least one of the following criteria: 1) is a novel variant 2) is a rare variant listed in MITOMAP as a polymorphism, but not in mtDB, or reported in mtDB with a frequency ≤0.2% 3) is a rare variant reported in the literature or MITOMAP as a "mutation" based on a single family study or a single report without the functional evidence of pathogenicity
Benign variant	mtDNA variant reported in the MITOMAP database as a polymorphism, with no evidence of disease association in population or family studies and is reported in the mtDB with a frequency >0.2%

1.3.2 Mitochondrial diseases due to mtDNA mutations

The first association between mitochondrial dysfunction and a clinical phenotype was established in 1962 [21, 34]. Since then, a variety of mitochondrial defects have been described. Mitochondrial diseases are multisystem diseases characterized by defects in the assembly and function of the mitochondrial respiratory chain. Mutations of both the mitochondrial DNA (mtDNA) and nuclear DNA (nDNA) have been identified as leading causes of these diseases, amounting to a combined prevalence of adult mitochondrial disease of ~1 in 4,300 [35]. As discussed, the vast majority of mitochondrial proteins are encoded by the nDNA, therefore diseases caused by mutations in these genes may be inherited in an autosomal dominant, autosomal recessive or X-linked manner [36]. Furthermore, age-

associated neurodegeneration such as in Parkinson`s and Alzheimer`s disease as well as physiological aging itself have been associated with mitochondrial dysfunction [37]. Mitochondrial diseases due to mutations of nuclear genes in the respiratory chain represent the minority of diagnosed mitochondrial disease, however increasingly more nDNA gene defects continue to be identified [38]. Considering mtDNA mutations, to date, more than 150 mtDNA mutations are known to have medical significance. One of the commonly used classifications of mitochondrial diseases caused by mtDNA mutations has arisen from recent advances in molecular genetics as displayed (**Table 1.2**) [39].

The point mutations of mtDNA are generally maternally inherited, this includes tRNA, rRNA and protein genes. More than half of disease-related point mutations are found in the tRNA genes, which make up less than ten percent of the mitochondrial genome [40]. Common diseases resulting from the point mutations in tRNA genes are MERRF and MELAS, in which the tRNA-Lys and tRNA-Leu genes are disrupted, respectively. A classic example of single-nucleotide mutations in-protein-coding genes is Leigh syndrome, characterized by psychomotor developmental delay, ataxia, and muscular hypotonia, with a point mutation in the ATPase 6 (*MT-ATP6*) gene, encoding a subunit of complex V of the respiratory chain.

Table 1.2: Genetic classification of mitochondrial diseases caused by mtDNA mutations

Point mutations in protein-coding genes	• Protein-coding genes • Leber hereditary optic neuropathy (LHON) (m.11778G>A, m.14484T>C, m.3460G>A) • Neurogenic weakness with ataxia and retinitis pigmentosa/Leigh syndrome (m.8993T>G, m.8993T>C)
Point mutations in tRNA genes	• Mitochondrial encephalomyopathy with lactic acidosis and stroke-like episodes (MELAS) (m.3243A>G, m.3271T>C, m.3251A>G) • Myoclonic epilepsy with ragged red fibers (MERRF) (m.8344A>G, m.8356T>C) • Chronic progressive external ophthalmoplegia (CPEO) (m.3243A>G, m.4274T>C) • Myopathy (m.14709T>C, m.12320A>G) • Cardiomyopathy (m.3243A>G, m.4269A>G) • Diabetes and deafness (m.3243A>G, m.12258C>A) • Encephalomyopathy (m.1606G>A, m.10010T>C) • Nonsyndromic sensorineural deafness (m.7445A>G)
Point mutation in rRNA genes	• Aminoglycoside-induced nonsyndromic deafness (m.1555A>G)
Rearrangements (deletions & duplications)	• Chronic progressive external ophthalmoplegia (CPEO) • Kearns-Sayre syndrome (KSS) • Diabetes and deafness

Despite the multitude of pathogenic mutations, clinical manifestations of mitochondrial disease are often very similar. In general, clinical manifestations occur in tissues and organs which are heavily dependent on the respiratory chain due to their high metabolic demands, such as the brain, muscle and heart. Neurological phenotypes and muscular phenotype such as myopathy have significant morbidity in this disease group, however cardiac, ophthalmic and endocrine systems are also frequently involved [41]. As discussed, the mtDNA mutations can

be homoplasmic or heteroplasmic and therefore the severity of the mitochondrial defects is influenced by the degree of heteroplasmy.

The germ-line transmission of mutated mtDNA is by the maternal lineage. The amount of mutated mtDNA transmitted to the offspring is variable and is determined by the "genetic bottleneck" [42]. This concept was originally illustrated in the maternal lineage of Holstein cows in 1980 [43], however the mechanisms remain unclear. The egg cell contains a high number of mitochondria, with the possibility that some of the mtDNA molecules are mutated. During early oogenesis, the number of mtDNA molecules is greatly reduced and a number are selectively transferred into each oocyte. Depending on the degree of heteroplasmy of the egg, a random shift of mtDNA mutational load of the embryo is determined [44]. Similar to sporadic mutations, a single mtDNA molecule can mutate during mitoses of early oogenesis or embryogenesis and depending on the time and the affected cell, this event leads to the distribution of a different degree of heteroplasmy across the somatic cells and subsequent dysfunction of the affected organs or tissues. The type of the affected cells in the early stages of development result in the mosaic-like distribution in the histomorphology.

In most mtDNA-associated mitochondrial diseases, such as CPEO, MELAS and MERRF, skeletal muscle shows a pathological mosaicism of metabolically compensated and noncompensated fibers. The mosaic is apparent using histochemical stains, typically with combined cytochrome c oxidase/succinate dehydrogenase (COX/SDH) staining. This is a common diagnostic test, whereby decompensated fibers are negative for the activity of complex IV of the respiratory chain, cytochrome c oxidase (COX-) but retain the blue (SDH) stain, which reflects the activity of the nuclear-encoded complex II of the respiratory chain (succinate–ubiquinone oxidoreductase). As discussed, complex II is the only respiratory complex entirely encoded by nuclear DNA, therefore the SDH stain is unaffected by deleterious mutations of mtDNA and is thus a reliable marker of mitochondrial abundance. Compensated fibers stain orange as a result of a functioning complex IV.

It is clear that the level of mutated mtDNA can alter over the course of a lifetime. A mathematical model of human mtDNA replication, "relaxed replication of mtDNA", provides an explanation for the late-onset of some mitochondrial diseases [45]. The model describes that changes of the proportion of mutant mtDNA in post-mitotic tissues are due to the different rates between the replication of mutant mtDNA and of wild-type (wt) mtDNA, which can subsequently affect the threshold of mutant copies. For instance, mtDNA with large-scale deletions could have an advantage on repopulating cells over wt mtDNA. Another process termed "mitotic segregation" might explain the change in mitotic tissue. In a heteroplasmic state, the cell randomly transmits the mutated and non-mutated mitochondria between the daughter cells [46]. Therefore, mutation load is variable from one cell generation to the next, which will result in a mutational load at or below the pathogenic threshold over time. The clinical syndromes associated with mtDNA mutations are therefore extremely variable in presentation and can occur at any age.

1.3.3 Pathophysiological effects of mtDNA mutations

The expression of mtDNA is indispensable for mitochondrial oxidative phosphorylation (OXPHOS), therefore, the primary response to mtDNA mutations is the decline of cellular energy production. A large number of pathogenic mtDNA variants detrimentally influence the activity of electron transport chain and ATP synthesis. Furthermore, mutations of mtDNA have several adverse effects on mitochondrial dynamics and induce inflammasome activation to disrupt the mitochondrial homeostasis and inflammatory response.

Mitochondria are dynamic reticular organelles with high plasticity of structures, as they undergo constant fission and fusion. These dynamic processes regulate mitochondrial homeostasis and maintain mitochondrial function by segregating the destroyed mitochondria via the fission process and facilitating mitochondrial remodeling, rearrangement and proliferation via the fusion process [47, 48]. Consequently, mitochondria can respond rapidly to cellular energy demands, whether adapting to the physiological or environmental changes.

In mammalian cells, mitochondrial fusion is mediated by the fusion relevant proteins mitofusin 1 (Mfn1) and 2 (Mfn2) as well as optic atrophy protein 1 (OPA1) (**Figure 1.3A**). Mfn1, Mfn2 and OPA1 are dynamin-related GTPases responsible for the mitochondrial fusion process of the outer and inner mitochondrial membranes, respectively. Meanwhile, a fraction of Mfn2 is also found in the endoplasmic reticulum (ER), regulating ER morphology, bridging mitochondria and ER, and facilitating mitochondrial uptake of calcium from ER stores [49]. OPA1 is necessary to retain mitochondrial genomes and control apoptosis, while, downregulation of OPA1 can result in aberrant cristae remodeling and the release of cytochrome c [50-53]. Mutations in Mfn2 and OPA1 have been reported in patients with multisystem clinical symptoms, including progressive external ophthalmoplegia and autosomal dominant optic atrophy (ADOA), with mtDNA large deletions in skeletal muscle [54-56]. Moreover, it has been confirmed by the study in yeast that fusion deficient mutants show defects of the respiration chain and failure to maintain the mitochondrial genome [57, 58].

Fission is mediated by another cytosolic GTPase, dynamin-related protein 1 (Drp1), which tethers to the fission proteins (such as hFis1) anchored in the mitochondrial outer membrane (**Figure 1.3B**) [59]. Fission is directly correlated with efficient mitochondrial transport and apoptosis. A number of studies show that mitochondrial fragmentation leads to apoptosis through the Drp1-dependent pathway in many organisms. Additionally, Bax, a pro-apoptotic Bcl-2 family member, interacts with Mfn1, Mfn2 and Drp1, providing support for the association between apoptosis and mitochondrial dynamics [60, 61]. Waterham et al. reported a mutation in the Drp1 gene resulting in abnormal brain development and lethality due to the fission defect [62]. Furthermore, Lipton reported that S-nitrosylated Drp1 (SNO-Drp1) affected amyloid-β (Aβ)-induced excessive mitochondrial fission and contributed to neuronal death and synaptic loss [63].

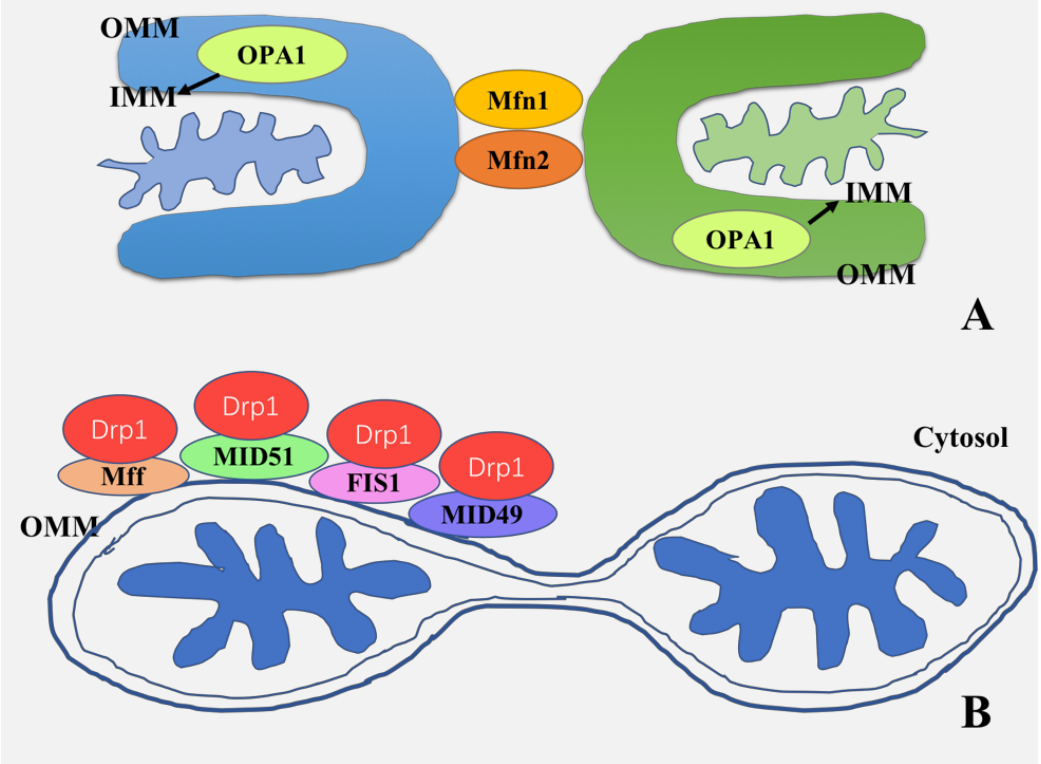

Figure 1.3: Mitochondrial fusion and fission in mammalian cells. (A) Mitochondrial fusion requires dynamin-related GTPase proteins Mfn1 and Mfn2, located in the outer mitochondria membrane (OMM), in addition to OPA1, located in the inner mitochondria membrane (IMM). (B) Mitochondrial fission is mediated by cytosolic dynamin-related protein 1 (Drp1). Drp1 is also a GTPase protein, which tethers to four fission proteins (Mff, Fis1, MID49, MID51) anchored in the OMM.

Inflammasomes are cytosolic multiprotein complexes formed in response to pathogenic microbes and physiological stimuli to activate proinflammatory caspases such as caspase-1, facilitating the maturation and secretion of interleukin-1β (IL-1β) and IL-18 [64]. The essential components of the inflammasome complexes contain nucleotide-binding domain and leucine-rich repeat containing proteins 1 (NLRP1), NLRP3 and NLRC4, which belong to the NOD-like receptor (NLR) family, and the effector molecule caspase-1, as well as the apoptosis-associated speck-like adaptor protein (ASC). NLRP3 is the most intensively studied component of the inflammasome complex and integrates with the adaptor ASC protein and procaspase-1 to form the NLRP3 complex. It is reported that NLRP3 inflammasomes produce mature IL-1β in the presence of signal 1 (often NF-κB) owing to activation caused by mitochondrial apoptotic signaling [65]. Aggregated β-amyloid and extracellular ATP can also

activate the NLRP3 inflammasome and additionally induce mitochondrial apoptosis and damage leading to the release of oxidized mtDNA into the cytoplasm [66]. Furthermore, Shimada et al. reported oxidized mtDNA, which was generated and released into the cytoplasm due to ROS production and K+ efflux, to serve as a NLRP3 direct activator to drive inflammasome assembly [65]. It remains unclear how exactly the oxidized mtDNA triggers the NLPR3 inflammasome, but it is speculated that the Ca^{2+} signaling maybe act as an intermediate step to promote the activation of NLPR3 complex [67].

1.3.4 Defense mechanisms against mtDNA mutations

Mitochondrial quality control is crucial to maintain mitochondrial function and cellular homeostasis [68-70]. During aging, mitochondrial and nuclear genomes accumulate mutations that impair the mitochondria. Mitochondrial quality control therefore removes the dysfunctional mitochondria and prevents the onset of mitochondrial disease.

Primary mechanisms for mitochondrial quality control are three-fold and relate to the removal of the damaged proteins or of the damaged organelle. The first mechanism is concerned with the core process for damaged protein degradation within mitochondria which hinges on the ubiquitin–proteasome system (UPS). As the energy factories of the cell, mitochondria are exposed to high levels of ROS production which can damage protein structure and affect protein folding. The mitochondrial unfolded protein response (UPRmt) is triggered by the accumulation of unfolded or misfolded proteins in the mitochondria leading to elevation of mitochondrial chaperone proteins (such as chaperonin heat shock protein 60 (HSP60) and HSP70) and proteases (such as ClpP), which ensure the proper folding of misfolded proteins or mediate damaged protein degradation, respectively [71]. UPS can eliminate misfolded, oxidized or denatured mitochondrial proteins embedded in the outer mitochondrial membrane [72]. The second mechanism is concerned with mitochondrial morphology and dynamic fission-fusion events to compensate for damaged mitochondria at the organelle level as the mitochondria are constantly fragmenting and fusing with a steadily regulated manner [57, 73] . The third mechanism concerns removal of the damaged organelles by a process of autophagy,

more precisely termed mitophagy in the setting of the mitochondria. In mitophagy, when mitochondrial defects reach the damage threshold, the process of fusion becomes blocked and the mitochondrion as a whole is eliminated via selective autophagy [74]. The term autophagy is defined as the degradation of cytosolic components and organelles within lysosomes [75]. Recent studies have indicated that the interplay between mitochondrial autophagy with the mitochondrial function is a responsible mechanism underlying neurodegenerative disease. As mitophagy is a major mitochondrial quality control mechanism, playing an important role in cellular adaption to oxidative stress, it is not surprising that dysregulation of mitophagy is relevant to neurodegenerative diseases, which in turn are associated with mitochondrial dysfunction caused by mtDNA mutations [76]. Mitophagy deficiencies lead to the accumulation of dysfunctional mitochondria, promoting excessive ROS generation and cytosolic transmission of mtDNA, resulting in inflammatory activation [77].

1.4 Mitochondrial proteomics

Proteomics is a high-throughput and large-scale method for identification and quantification of proteins within a biological unit such a cells, tissues or organisms, providing a link between genotype and phenotype. The first study of mitochondrial proteomics was described in 1998 [78]. Over the last 20 years, the human mitochondrial proteome has been mapped and defined, detecting more than 1,000 mitochondrial proteins encoded by both the mitochondrial genome and the nuclear genome [79]. Since the mitochondria participate in a plethora of pathological and physiological processes, the investigation of alterations of the mitochondrial proteome is beneficial to clarify the pathogenic mechanisms of numerous human diseases. At present, the focus of mitochondrial proteomics research is on the verification of all of the mitochondrial protein components within a single sample and their post-translational modifications (PTMs) in order to develop an integrated mitochondrial proteome database. In addition, the study of comparative mitochondrial proteomics aims to explore the differentially expressed mitochondrial proteins in abnormal samples or under special states in favor of revealing the pathogenesis of mitochondrial diseases.

Mitochondrial proteomics has been a “hot topic” for the past decade, as mitochondria represent a hub of cellular signaling activity and pathways involved in disease pathogenic mechanisms associated with a wide disease spectrum [68, 80-82] and with the physiological aging process [83, 84]. There is however only limited availability of sufficient samples from human tissues for proteome analyses due to strict medical and ethical issues. The continuous development in the methods of sample preparation and sensitivity and accuracy of mass spectrometry analysis techniques however allows examination of small, more readily available biopsy samples to be realized. This produces valuable information on pathology through direct proteomics analysis of affected disease-associated material.

1.4.1 Techniques for mitochondrial proteomics

The identification of differential proteomics is most frequently accomplished by two-dimensional gel electrophoresis (2DE) and mass spectrometry (MS). For studies of mitochondrial proteomics, the most direct technique is to identify mitochondrial proteins in purified fractions of mitochondria from samples by MS. 2DE-based proteomic analysis is however unable to visualize low-abundant proteins, owing to the difficulty in separating hydrophobic proteins and proteins with the extreme isoelectric point or molecular weights, such as membrane proteins [85]. To date, methods have been explored to perform the separation of hydrophobic proteins, including transmembrane domain (TM) proteins, such as sodium dodecyl sulphate-polyacrylamide gel electrophoresis (SDS-PAGE), benzyldimethyln-hexadecylammonium chloride (16-BAC)/SDS-PAGE and cetyl trimethylammonium bromide (CTAB)/SDS-PAGE [86]. With the development of electrospray ionisation (ESI), liquid chromatography coupled with MS (LC-MS) arose as a powerful technique with high sensitivity and specificity which facilitates protein quantification using stable isotope labeling (in vitro and in vivo), as well as avoiding the limitation of low dynamic range due to gel staining. Quantitative proteomic analyses can be accomplished through gel-free isotope labeling approaches such as isotope-coded affinity tags (ICATs) [87], stable isotope labeling with amino acids in cell culture (SILAC) [88], isobaric tags for relative and absolute quantitation (iTRAQ) [89] and enzymatically with ^{18}O during

proteolytic digestion, for accurate determination of the amount of each protein [90]. MS-based quantitative proteomics has the capability to incorporate large amounts of phenotypic information in relation to protein expression, interactions and post-translational modifications [91].

Liquid chromatography-mass spectrometry (LC-MS) instruments now enable the identification of proteins and peptides at extremely low levels. The completion of such "microproteomics" relies on a modified technique for microgram-quantities of sample and on effective sample processing. Thus, sample size and complexity should be given more attention in LC-MS. MS analysis should preferably be carried out in affected tissues such as skeletal muscle, a predominant target tissue in mitochondrial disease [92]. However, since the vast majority of muscle mass consists of large and highly abundant sarcomeric proteins, skeletal muscle is technically challenging for mass spectrometry [93]. Laser capture microdissection (LCM) is a useful technique that allows for pure isolation of the cells of interest or anatomical regions of tissue from sample sections [94, 95]. Banded with immunohistochemistry, LCM can remove targeted cell types according to a specific histological stain or protein marker, thus cells of interest can be extracted and identified without the interference of adjacent tissue structures. The verification of peptide–spectrum assignments should be checked carefully. Software tools available to automatically analyze the tandem mass spectrometry datasets include Trans-Proteomic pipeline (TPP), Census™ [96] and MaxQuant™ [97].

1.4.2 Applications of mitochondrial proteomics

Mitochondrial proteomics have been widely applied to illuminate molecular alterations responsible for the pathogenesis of mitochondrial diseases at the protein level through large scale proteomics analyses. The identification of mitochondrial disease-causing proteins contributes not only to the comprehension of molecular signaling pathways associated with mitochondrial and mitochondrial-related diseases but also to the discovery of potential therapeutic targets. Considering that most mitochondrial proteins are encoded by nDNA and

not the mtDNA, the study of mitochondrial mechanisms should make an alliance between proteomic and genomic data. Rabilloud et al. applied comparative proteomics to describe the effects of mutations in mitochondrial tRNA genes on the steady-state level of mitochondrial protein encoded by nDNA [98]. A similar proteomic approach was used to compare wild-type with MERRF mitochondria from sibling human cybrid cell lines and performed a quantitative analysis [99]. Furthermore, a study performing quantitative mitochondrial proteomics showed that acyl-CoA dehydrogenase short chain (ACADS) deficiency had a widespread influence on fatty acid beta-oxidation [100]. Taking all of the above factors into account, mitochondrial proteomics will beyond doubt supply useful information for various mitochondrial related studies.

As mentioned in **1.3.2**, pathological mtDNA mutation mosaicism is superimposed onto the physiological mosaicism of different fiber types which characterizes skeletal muscle, one slow-type 1 and two fast-type 2 (2A and 2X, three in rodents which also have 2B fibers), each with specific contractile and metabolic properties. In humans, slow fibers have more abundant mitochondria than fast fibers. Using MS-based proteomics, related study has previously shown that human fast and slow fibers undergo different changes during the process of aging [101].

2. Objective

This study utilizes the combination of laser capture microdissection (LCM) and quantitative proteomics to investigate novel pathogenic mechanisms of mitochondrial diseases at the level of individual muscle fibers. The mosaicism of COX+ and COX- fibers in mtDNA-related diseases provides a unique opportunity to reveal mitochondrial disease mechanisms at the cellular level. Based on this objective, a LCM-based proteomic workflow is performed to excise the pure cells of COX+ and COX- fibers from frozen muscle biopsies of CPEO patients, followed by a rapid and deep proteome analysis. Since LCM enables microsampling, our LCM-based proteomic workflow requires only little tissue, in the ng range, to yield quantitative data on thousands of proteins. Comprehensive knowledge of proteomic analyses in individual COX+ and COX- fibers can illuminate the pathogenesis of mitochondrial disease and reveal the fiber type-specific adaptive molecular responses to mitochondrial dysfunction.

3. Materials and Methods

3.1 Ethical Statement

The research project was approved by the ethics committee of the LMU Munich and the study has been performed in accordance with the ethical standards laid down in the 1964 Declaration of Helsinki and its subsequent amendments. Muscle biopsies were obtained for diagnostic purposes and written informed consent for using parts of it for research purposes was obtained from patients or their legal guardians.

3.2 Patients

All muscle specimens and myoblast cells were obtained from the biobank of the German network for mitochondrial diseases (mitoNET) at the Friedrich-Baur-Institute. We randomly selected 3 patients with CPEO, defined by the pathognomonic clinical phenotype of the presence of ragged red fibers (RRF) on muscle biopsy and the detection of an mtDNA deletion (**Table 3.1**). Patient 1 is a male German patient who developed ptosis and progressive external opthalmoplegia (PEO) with double vision from the age of 16. From the age of 39, he complained of mild muscle weakness of the upper and lower extremities. The diagnosis of CPEO was confirmed by muscle biopsy showing RRF and COX- fibers in addition to a 5 kb mtDNA single deletion (common deletion) in 50% of mtDNA molecules. Patient 2 is a female Turkish patient who developed ptosis and PEO from the age of 20. From the age of 32, she complained of mild muscle pain and weakness of the upper and lower extremities. The diagnosis of CPEO was confirmed by muscle biopsy showing RRF and COX- fibers in addition to a 6 kb mtDNA single deletion in 50% of mtDNA molecules. Patient 3 is a male German patient who developed ptosis and PEO with double vision from the age of 34. He did not suffer from muscle weakness of the upper and lower extremities. The diagnosis of CPEO was confirmed by muscle biopsy showing RRF and COX- fibers in addition to a 5 kb mtDNA single deletion (common deletion) in 50% of mtDNA molecules.

Diagnostic fragments of the right deltoid or left quadriceps muscle were collected by open muscle biopsy. Muscle specimens were then immediately frozen in liquid nitrogen and stored at -80°C. The control myoblast cells were randomly selected from 3 patients with no known mitochondrial disease.

Table 3.1: Basic characteristics of the study participants.

CPEO	Race	Sex	Age at biopsy (yrs)	Size / heteroplasmy of single mtDNA deletion	Phenotype
Patient 1	European-Caucasian	Male	38	5 kb / 50%	CPEO
Patient 2	European-Caucasian	Female	32	6 kb / 50%	CPEO
Patient 3	European-Caucasian	Male	49	5 kb / 50%	CPEO

3.3 Histochemistry

3.3.1 Tissue preparation for cryosectioning

Muscle specimens were transferred in liquid nitrogen to the cryostat. Alternate serial sections (10 μm) were adhered to Superfrost plus microscope slides for histochemical staining and to membrane slides for laser microdissection. Superfrost plus slides were air-dried for ~24h and then stored at -20°C for the next histochemical staining. Membrane slides were stored at -80°C prior to cutting and processing for MS-based proteomics.

Table 3.2: Consumables and equipment for tissue preparation

Consumables / equipment	Product number	Manufacturer
Leica Membrane Slides © PEN membrane 2.0µm	11505158	Micro Dissect Gmbh (Herborn)
Slides superfrost	7201277	Menzel GmbH + Co KG
Coverslips	190002450	IDL (Nidderau)
Cryostat 2800 Frigocut E	—	Reichert-Jung

3.3.2 Sequential cytochrome c oxidase / succinate dehydrogenase (COX/SDH) histochemistry

Slides were allowed to thaw and dry at room temperature for 1h and were processed according to standard protocols [102]. For COX staining, sections were incubated in cytochrome c oxidase medium (100 µM cytochrome c, 4 mM diaminobenzidine tetrahydrochloride, and 20 µg/ml catalase in 0.2 M phosphate buffer, pH 7.0) for 90 min at 37 °C. Sections were then washed in standard PBS, pH 7.4 (2 × 5 min) and incubated in succinate dehydrogenase (SDH) medium (130 mM sodium succinate, 200 µM phenazine methosulphate, 1 mM sodium azide, 1.5 mM nitroblue tetrazolium in 0.2 M phosphate buffer) for 120 min at 37 °C. Sections were then washed in PBS, pH 7.4 (2 × 5 min) and in double-distilled water (2 × 2 min) rinsed in distilled and dehydrated in an increasing ethanol series up to 100%, prior to incubation in xylene and mounting in Eukitt (**Table 3.3 and 3.4**).

Table 3.3: Chemicals for COX-SDH staining

Chemicals	Product Number	Manufacturer
Diaminobenzidine (DAB)	D-5637	Sigma
Cytochrome c	C-2506	Sigma
Sodium succinate	S-2378	Sigma
Nitro blue tetrazolium (NBT)	N-6876	Sigma
Phenazine methosulfate	P-9625	Sigma
Sodium azide	BDH30111	Sigma
Catalase	C-9322	Sigma
PBS	P0014 (0.2M, Ph7.5) P0008 (0.1M, Ph7.4)	Sigma-Aldrich

Table 3.4: Protocols for combined COX-SDH staining.

Preparations of samples	
	1. Thaw and dry at room temperatures for 1h
COX staining	
	2. 30mg cytochrome c, 30mg diaminobenzidine tetrahydrochloride add to 30ml 0.1M PBS 3. Adjust PH to 7.0 4. Add 20mg catalase to CCO solution 5. Incubate at 37 ° C for 90 mins
Wash	
	6. 5 mins in 0.2M PBS for 2 times
SDH staining	
	7. 6,12mg PMS add to 10ml 0,1M phosphate buffer, devide 3ml aliquots and store at -20 ° C 8. Make 0.2M Na-succinate solutions by mixing 2710mg sodium succinate with 50ml double-distilled water 9. 15ml 0.2M sodium succinate solutions, 40mg NBT add to15 ml 0.2M PBS 10. Incubate at 37 ° C for 120 mins
Wash	
	11. 5 mins in 0.2M PBS for 2 times 12. 2 mins in double-distilled water for 2 times
Decolorizer	
	14. Wash 30 secs in 75% alcohol 15. Wash 30 secs in 95% alcohol 16. Wash 30 secs in 99% alcohol for 2 times
Storage	
	18. Cover medium and coverslip

3.4 Laser capture microdissection (LCM)

In LCM, polyethylene naphthalate (PEN) membranes are necessary. These special microscope slides are coated with a thin transparent film on the surface of the glass slide that can be cut off by a weak laser beam [103]. By cutting off the marked area of the tissue, the cells of interest fall down and are collected in a prepared reaction vessel. The primary advantage of this membrane slide is that the PEN membrane provides great consistency in the process of capturing and collecting cells, which can ensure not only faster collection of large sections of samples but also less dependency on dehydration contributing to the complete removal of the sample from the slide.

Table 3.5: Consumables and laser capture microdissection device

Chemicals	Product Number	Manufacturer
PEN membrane slides	11505158	Leica
Leica LMD 7000 system	—	Leica
0.5ml Thermo-Tube	AB-0350	Thermo Scientific

The procedure was essentially carried out as described in the literature by Koob et al. [104]. The images of whole COX/SDH stained slides and sections of interest were acquired and stored using a Leica LMD 7000 System. Next, we observed the unstained serial sections under the microscope at various magnifications and compared with the pictures of stained sections individually. According to the recognizable histochemical features of COX+ and COX- cells, we determined the coordinates of their corresponding unstained cells and cut them by LCM. 100 COX+ and 100 COX- cells were collected for each patient. Similarly, we selected 3 COX+ and 3 COX- single fibers with clearly recognizable histochemical features for each patient, then obtained 20 COX+ or 20 COX- serial sections for each fiber separately. The whole procedure was precisely timed for each sample and carried out in less than 30 min at room temperature. Fiber sections were captured by cutting the region of interest onto the

caps of 0.5ml Thermo-Tube, which were carefully closed and immediately frozen in liquid nitrogen at the end of the procedure. Samples were stored at -80°C until used.

3.5 Sample preparation and high pH-reversed phase fractionation

Total muscle (62 mg) was crushed in liquid nitrogen using a pestle and mortar. Powdered muscle samples and myoblast cells (3x 106 cells) were resuspended in 310 µl (5 µl/mg) and 200 µl SDC reduction and alkylation buffer, respectively. Samples were further boiled for 10 minutes to denature proteins [105]. The total muscle sample was further mixed (six times 30 seconds and cooled on ice in between) using a FastPrep®-24 Instrument (MP Biomedicals). Protein concentration was measured using the Tryptophan assay and 250 µg were digested overnight with Lys-C and trypsin in a 1:25 ratio (µg of enzyme to µg of protein) at 37 ºC, under continuous stirring at 1700 rpm. On the following day, samples were sonicated using a Bioruptor (Diagenode, 15 cycles of 30 sec) and further digested for 3 hours with Lys-C and trypsin (1:100 ratio). Peptides were acidified to a final concentration of 0.1% trifluoroacetic acid (TFA) for SDB-RPS (Polystyrene-divinylbenzene copolymer partially modified with sulfonic acid) binding and 40 µg of peptides were loaded on four 14-gauge Stage-Tip plugs (**Figure 3.1**). Peptides were washed first with isopropanol / 1%TFA (200 µl) and then 0.2% TFA (200 µl) using an in-house Stage-Tip centrifuge at 2000 x g. Peptides were eluted with 60 µl of elution buffer (80% acetonitrile / 1% ammonia) into auto sampler vials and dried at 60 C using a SpeedVac centrifuge (Eppendorf, Concentrator plus). Peptides were resuspended in 2% acetonitrile / 0.1% TFA and sonicated (Branson Ultrasonics, Ultrasonics Cleaner Model 2510) before peptide concentration estimation using the Nanodrop. About 40 µg of peptides of each sample were further fractionated into 54 fractions by the Spider fractionator device, which is under commercial development by PreOmics GmbH, Martinsried, Germany, with a rotor valve shift of 90 s and concatenated into 16 fractions using high pH reversed-phase fractionation, as previously described [106].

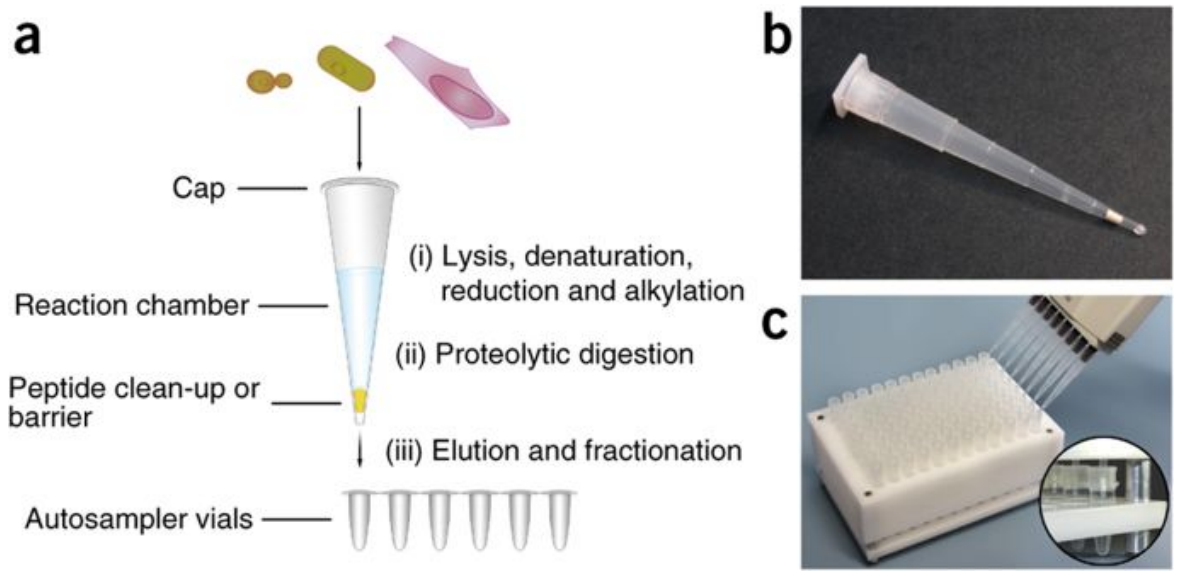

Figure 3.1: Protocol of minimal sample-processing completed in an enclosed volume [108]. (a) Profile of the in-StageTip (iST) sample-processing method. Protein material are directly transferred into a StageTip and are processed in three steps. (b) Enclosed iST reactor. (c) 96-well iST device for sample processing. Inset, shows StageTips reaching into

Table 3.6 Buffers used for iST

Lysis buffer	1% (w/v) SDC, 10mM TCEP, 40mM CAA, 100mM Tris pH8.5
Dilution buffer	milliQ Water (LysC - 1:10, Trypsin - 1:10, Lysate : Buffer)
Loading buffer (SDB-RPS)	50% (v/v) Ethyl acetate, 0.5% (v/v) TFA (1:2)
Washing buffer (SDB-RPS)	1. 50 µl 100% (v/v) Ethyl acetate, 50 µl 0.2% (v/v) TFA 2. 100 µl 0.2% (v/v) TFA

3.6 Liquid Chromatography Tandem Mass Spectrometry (LC-MS/MS) analysis

Nanoflow LC-MS/MS analysis of tryptic peptides was conducted on a Q Exactive HF Orbitrap (Thermo Fisher Scientific) coupled to an EASYnLC 1200 ultra-high-pressure system (Thermo Fisher Scientific) via a nano-electrospray ion source (Thermo Fisher Scientific). Peptides were loaded on a 50 cm HPLC-column (75 µm inner diameter; in-house packed

using ReproSil-Pur C18-AQ 1.9 µm silica beads; Dr. Maisch). Peptides were separated using a linear gradient from 2% B to 20% B in 55 minutes and stepped up to 40% in 40 minutes followed by a 5 minute wash at 98% B at 350 nl/min where solvent A was 0.1% formic acid in water and solvent B was 80% acetonitrile and 0.1% formic acid in water. The gradient was followed by a 5 min 98% B wash and the total duration of the run was 100 minutes. Column temperature was kept at 60 C by a Peltier element-containing, in-house developed oven.

The mass spectrometer was operated in "top-15" data-dependent mode, collecting MS spectra in the orbitrap mass analyzer (60,000 resolution, 300-1,650 m/z range) with an automatic gain control (AGC) target of 3E6 and a maximum ion injection time of 25 ms. The most intense ions from the full scan were isolated with an isolation width of 1.5 m/z. Following higher-energy collisional dissociation (HCD), MS/MS spectra were collected in the orbitrap (15,000 resolution) with an AGC target of 5E4 and a maximum ion injection time of 60 ms. Precursor dynamic exclusion was enabled with a duration of 30 seconds.

3.7 Computational proteomics

The MaxQuant software (version 1.5.4.3) was used for the analysis of raw files. Peak lists were searched against the human UniProt FASTA reference proteomes version of 2016 as well as against a common contaminants database using the Andromeda search engine [97, 107]. Carbamidomethyl was included in the search as a fixed modification, oxidation (M) and phospho (STY) as variable modifications. The FDR was set to 1% for both peptides (minimum length of 7 amino acids) and proteins and was calculated by searching a reverse database. Peptide identification was performed with an initial allowed precursor mass deviation up to 7 ppm and an allowed fragment mass deviation 20 ppm. For the relative quantification of MYH isoforms, only peptides unique to each isoform were used for protein quantification in MaxQuant. The relative expression of each MYH isoform is calculated as percent of the summed intensity of the four adult isoforms (MYH1, MYH2, MYH4, MYH7).

3.8 Bioinformatic and statistical analysis

The Perseus software (version 1.5.4.2), part of the MaxQuant environment [108] was used for data analysis and statistical analysis. Categorical annotations were provided in the form of UniProt Keywords, KEGG and Gene Ontology. Mitocarta2 scores were provided as numerical annotations and filtered for x>1. Label free quantification (MaxLFQ) was used for protein quantification in all experiments, using a Z score where indicated [109]. Student's T-test was performed using a p value of 0.05 for truncation. Normalization for mitochondrial content was performed by dividing expression values by the expression of citrate synthase. PCA and cluster analysis was performed in the Perseus software using logged expression values. Where indicated, missing values were imputed by using random numbers from a normal distribution to simulate the expression of low abundant proteins. We used a width parameter of 0.3 of the standard deviation of all values in the dataset with a down shift by 1.8 times this standard deviation. These parameters were empirically determined over many different proteomics data sets.

4. Results

4.1 Combining laser capture microdissection (LCM) and proteomics to study mechanisms of mitochondrial disorders

We performed a LCM-based quantitative proteomic analysis approach for mitochondrial proteins that contribute to the pathogenesis of mitochondrial disorders. This LCM-based proteomic work flow consists of four major steps (**Figure 4.1**). The first step is to harvest COX+ and COX- cells from frozen muscle tissue specimens. The LCM allows for a more precise collection of interesting cells not only in the whole muscle samples but also in the single muscle fiber. The second step involves samples preparation by the in-StageTip method [105], which allows sample processing in a single reaction vessel to minimize sample loss, contamination, handling time and to increase quantification accuracy. The third step contains the measurement of high sensitivity, sequencing speed, and mass accuracy using a quadrupole - Orbitrap mass spectrometer (QExactive HF), and rapid qualitation, quantitation and statistical analysis of multiple proteins[110]. For the identification of proteins with low expression, we first built a fixed resource consisting of deep human skeletal muscle proteomes as libraries of identified peptide features by single-shot MS analyses of individually excised 10 µm sections of the frozen muscle biopsies. Based on the "match between runs" feature of the MaxQuant analysis software [97, 111], we transferred identifications from the peptide libraries to the patients' samples[93]. The last step involves the comparative analysis between different samples to detect molecular markers or pathways which are associated with mechanisms of initiation and progression of mitochondrial diseases. A flow chart summarizing the LCM-based proteomic strategy is shown in **Fig 4.1**.

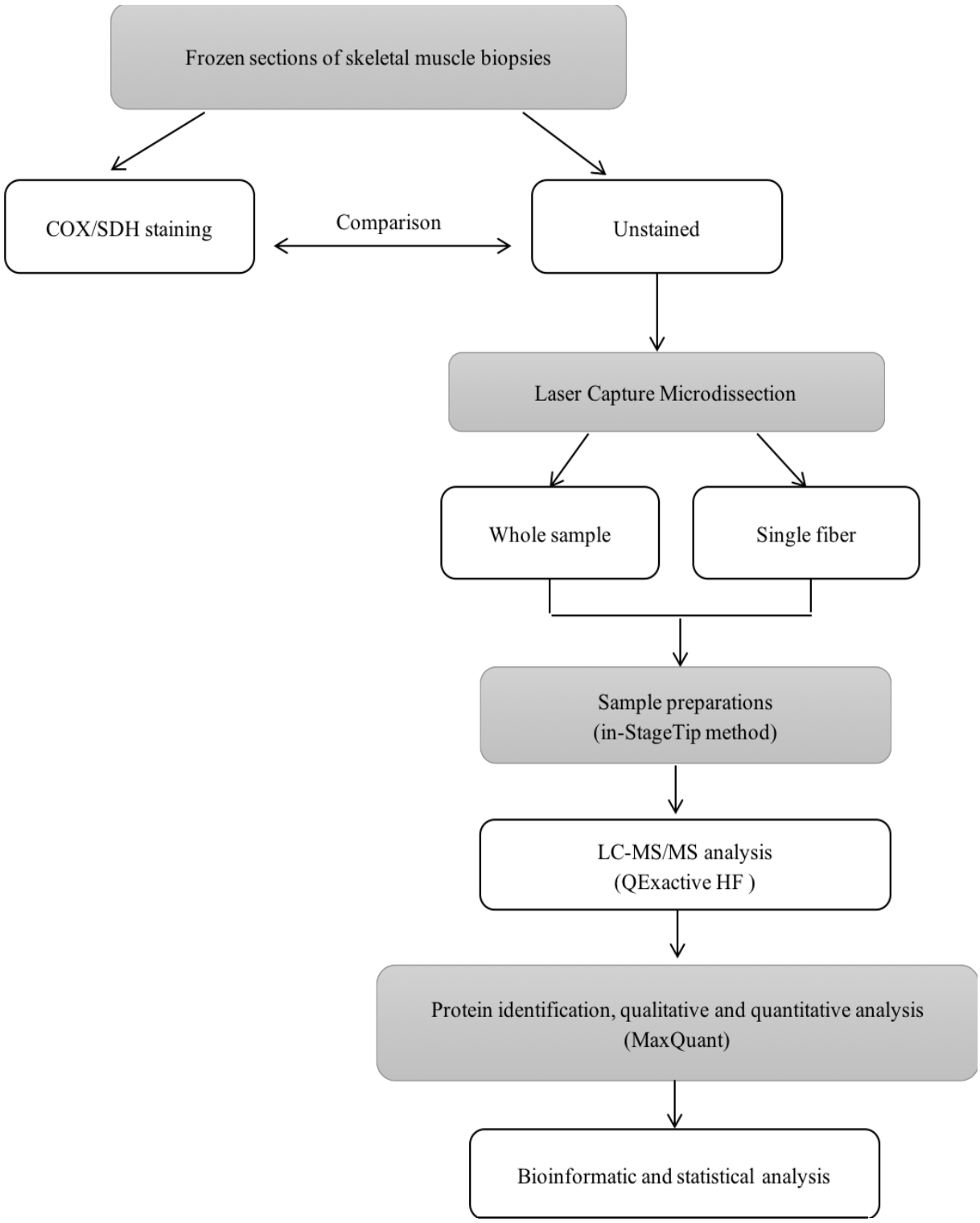

Figure 4.1: Outline of the LCM-based proteomic strategy to investigate mitochondrial diseases.

With our LCM-based proteomic strategy, triplicate proteome analyses of muscle sections from one patient can be carried out in 6 hours of total machine time and yield quantification of over 4000 proteins (**Figure 4.1.2 and 4.1.3**). The same strategy allowed the proteomic analysis of serial sections of single fibers, in which we quantified 2440 +/- 350 proteins on average (**Figure 4.1.3**).

Our library-based strategy triplicated protein identification with respect to direct sequencing by tandem mass spectrometry (MSMS). The advantage of this method was proportionally stronger in the dataset obtained by LCM of single muscle fibers, where peptides from low abundant proteins presumably fall below the intensity limit for identification by MSMS (**Figure 4.1.2**). The identification of proteins reached to 65% coverage of mitochondrial annotations according to our deep skeletal muscle libraries. Most of mitochondrial functional proteins, like proteins related with the respiratory chain and tricarboxylic acid (TCA) cycle, were mostly identified by MSMS.

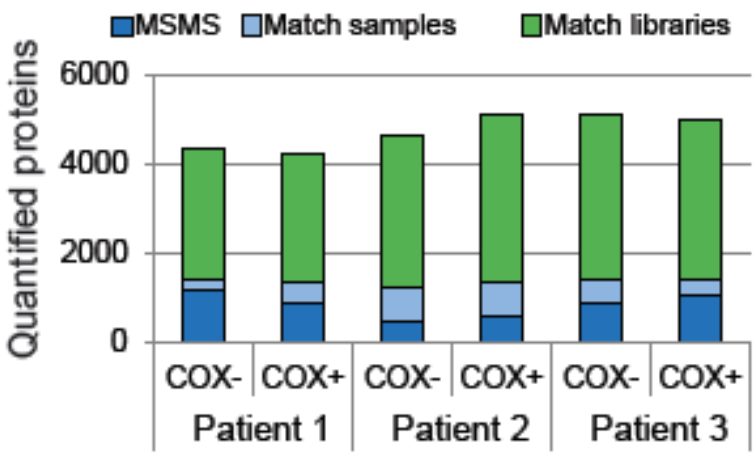

Figure 4.1.2: Number of proteins quantified for whole muscle samples of each patient.

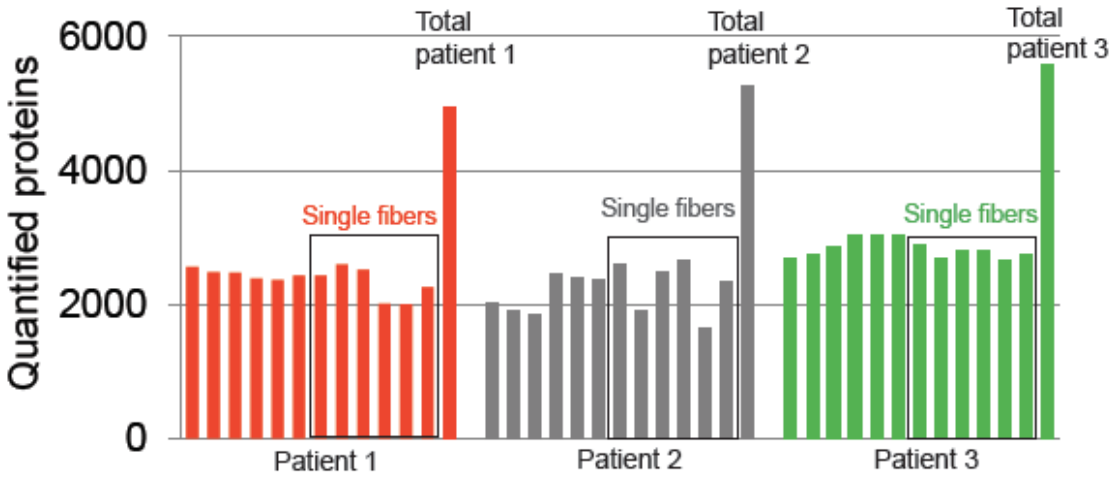

Figure 4.1.3: Number of proteins quantified for single muscle fibers of each patient.

4.2 LCM capture of skeletal muscle sections

In this study, we used frozen skeletal muscle biopsies of CPEO patients, in which a histochemical activity for COX/SDH staining showed a mosaic of brown (COX positive) and blue (COX negative) fibers (**Figure 4.2.1A**). Given the cellular histological distribution, LCM was used as a means to capture COX+ and COX- cells separately. Figure 4.2.1 shows pre- and post-microdissected tissue images and captured muscle cells. The infrared capture laser was applied to be as a microdissection instrument instead of the ultraviolet (UV) cutting laser, since the thermal energy provided by UV-laser approach could generate potential harm and lower protein harvest yields of interesting cells when cutting small cells or tissue fragments[112].

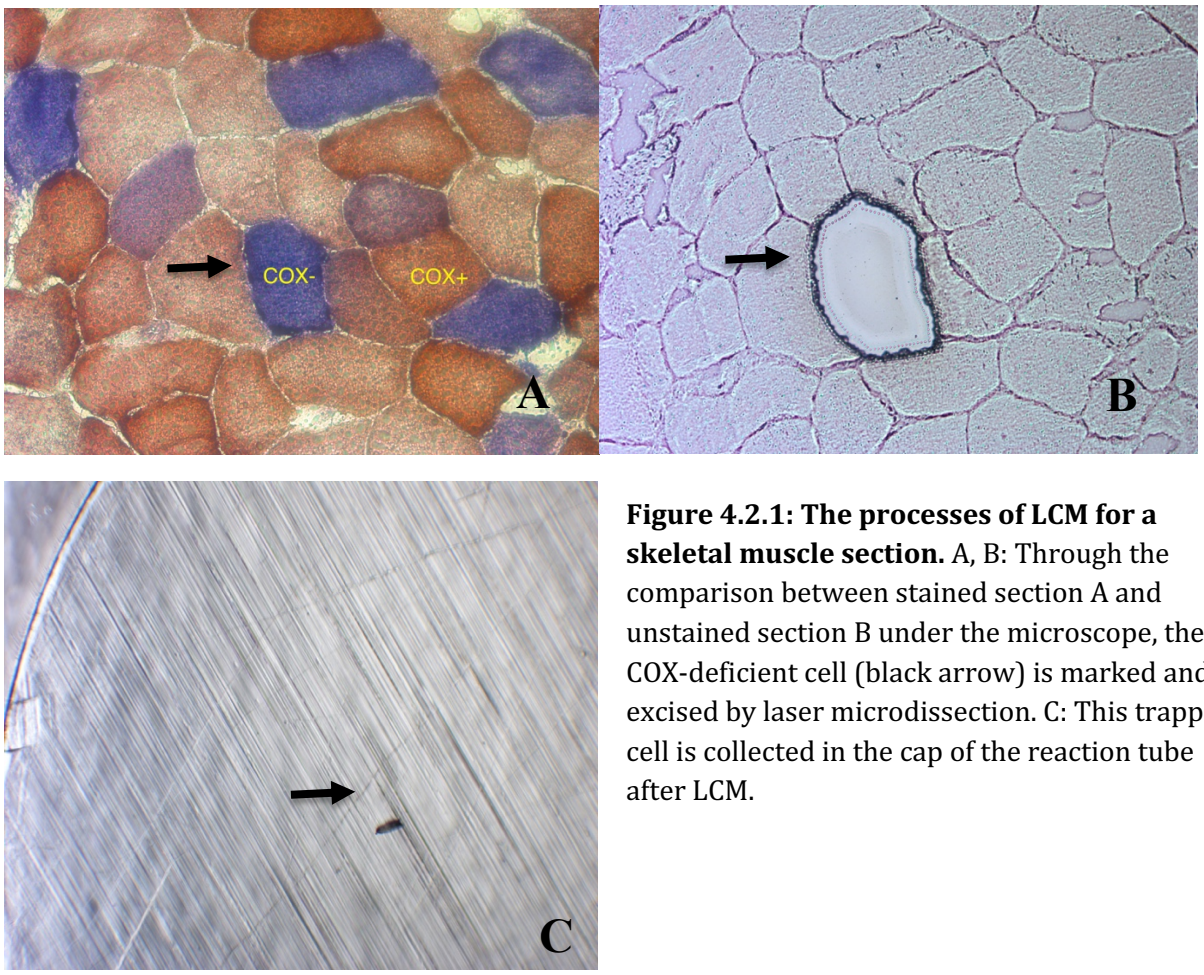

Figure 4.2.1: The processes of LCM for a skeletal muscle section. A, B: Through the comparison between stained section A and unstained section B under the microscope, the COX-deficient cell (black arrow) is marked and excised by laser microdissection. C: This trapped cell is collected in the cap of the reaction tube after LCM.

It is necessary that the sections of PEN membrane slides are exposed to very short air drying at room temperature to ensure a consistent and smooth cellular microdissection by LCM. Otherwise, excessive air drying or external moisture of sections would adversely impact on the separation of the plastic film from the glass slide. After the capture microdissection of individual fibers from 10 µm sections by LCM, we obtained separate pools of 100 COX+ and 100 COX- fibers from each of three CPEO patients. Using pools of muscle fiber sections helped to avoid sampling biases, such as different fiber type composition leading to different mitochondrial content. Besides, 20 COX+ and 20 COX- serial sections were cut in each fiber of selected 3 COX+ and 3 COX- single fibers for one patient separately.

4.3 Expression of respiratory complexes in COX+ and COX- muscle fibers

In this study, we quantified 73 out of 95 proteins annotated to the respiratory chain complexes and ATP synthase in humans (GO annotation). Then we differentiated the subunits of the respiratory chain complexes according to their gene localization in mtDNA (Figure 4.3.1, red boxes) and nDNA (Figure 4.3.1, black boxes), respectively, and analysed their differences in COX- and COX+ fiber pools.

For COX complex IV, all subunits showed more abundant in COX+ fibers compared to COX- fibers (**Figure 4.3.1A**), which serves as a proof of concept that the LCM-based proteomic approach reflects the significant diagnostic histochemical discrimination. This expression difference was strongly visible when we made analyses of the subunits of cytochrome oxidase (COX, complex IV) encoded by mtDNA. Further, we observed this for all respiratory chain subunits of mtDNA origin (**Figure 4.3.1**, right red boxes). Accordingly, COX+ muscle fibers of CPEO patients have been shown to contain more copies of mtDNA than the COX- counterparts [113]. Our study showed complex I subunits were significantly higher in COX+ than in COX- fibers (**Figure 4.3.1B**), however, complex III were essentially the same between COX+ and COX- fibers. Three out of four subunits of SDH (complex II), a histological marker of mitochondrial content, were more abundant in COX- fibers.

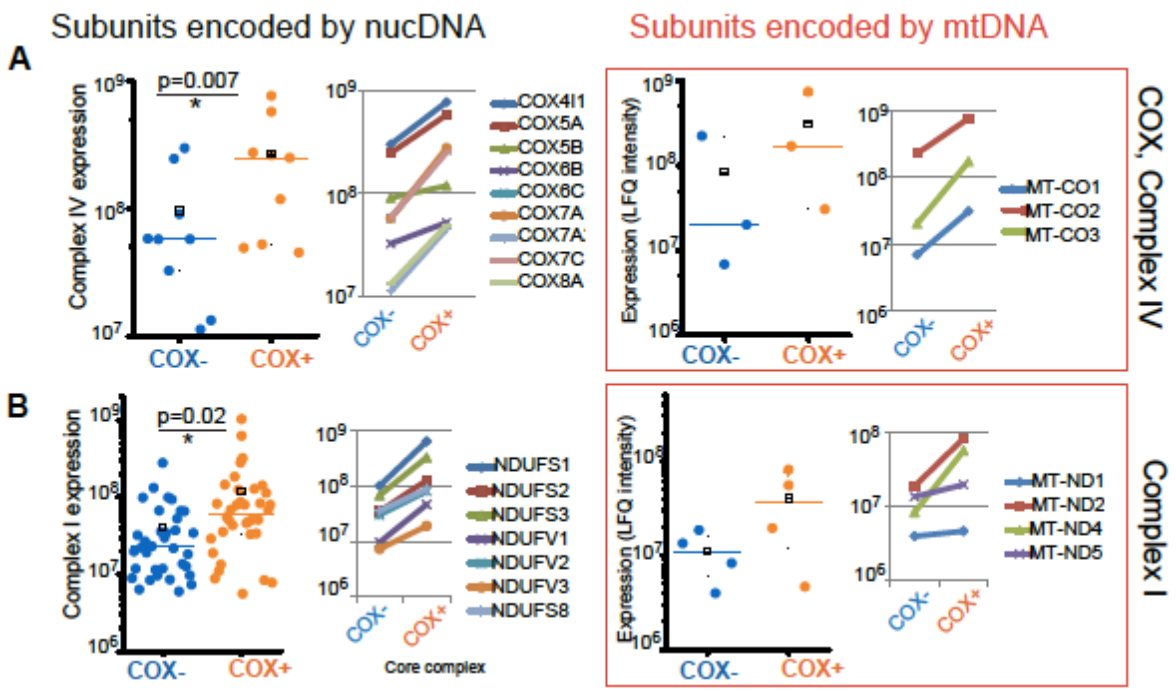

Figure 4.3.1: Expression of respiratory chain complexes IV and I in COX+ (orange) and COX- (blue) fibers. Boxplots are superimposed on the individual data points. Boxes show the mean, 25th and 75th percentile, whiskers show the standard deviation. A: Expression of COX (complex IV) subunits. B: Expression of complex I subunits. For simplicity, only the expression of the core catalytic complex is shown in the graph. (The median expression of each quantified protein of the complex in COX- and COX+ fibers is shown by the graph on the right of each boxplot. The values are log10 scaled.)

4.4 Potential molecular mechanisms of mitochondrial dysfunction at the cellular level

Through the comparison between the proteomes of COX+ and COX- fiber pools of three CPEO patients using a Student's t-test, the expression of 580 proteins exhibited significant statistic difference between the two groups ($p<0.05$). We performed a principal component analysis (PCA) for those significant mitochondrial proteins that showed a separation of the COX+ and COX- fiber pools along component 3 (**Figure 4.4.1A**). This process was driven by a specific enrichment of proteins annotated to the respiratory chain ($p<10^{-7}$) in COX+ fibers. In contrast, Figure 4.4.1B shows COX- fibers displaying a high expression of the fatty acid binding protein 5 (FABP5) and of Wolframin (WFS1) which as an endoplasmic reticulum (ER)- transmembrane protein participates in calcium homeostasis.

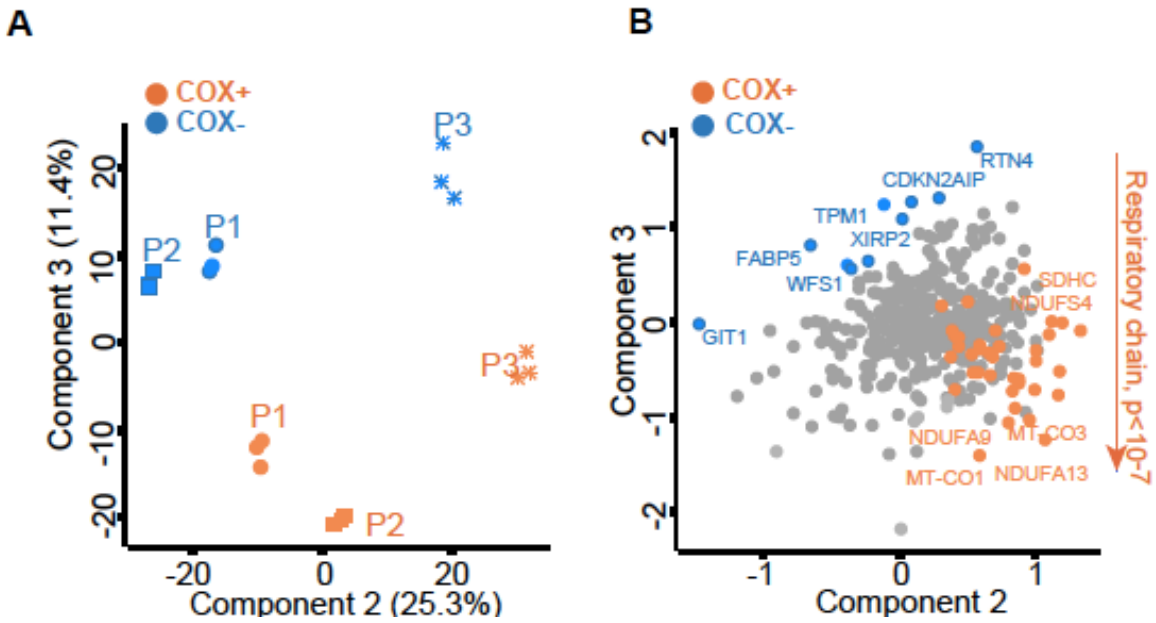

Figure 4.4.1: The separation of mitochondrial protein expression between the COX+ (orange) and COX- (blue) fiber pools. A: The separation showed in three CPEO patients. B: The separation showed in the highly significant enrichment of proteins annotated as respiratory chain in COX+ fibers.

Then, we used Mitocarta 2 [114] to select the mitochondrial proteins from the dataset. The expression of all mitochondrial proteins was normalized by CS expression, which would correct differences in mitochondrial content between patients and mitochondrial number between samples. It contributed to analyze the features of mitochondrial proteomes of COX+ and COX- fiber pools. 109 proteins showed a highly significant expression in COX+ fibers annotating by the respiratory chain and electron transport performing >40-fold enrichments (**Figure 4.4.2A**). 49 Proteins with higher expression in COX- fibers displayed significant enrichments (> 25-fold) in annotations related to mitochondrial translation (**Figure 4.4.2B**). The increased expression of mitochondrial translation proteins might be regarded as a potential compensatory mechanism to offset the dysfunction of the respiratory chain in COX- fibers.

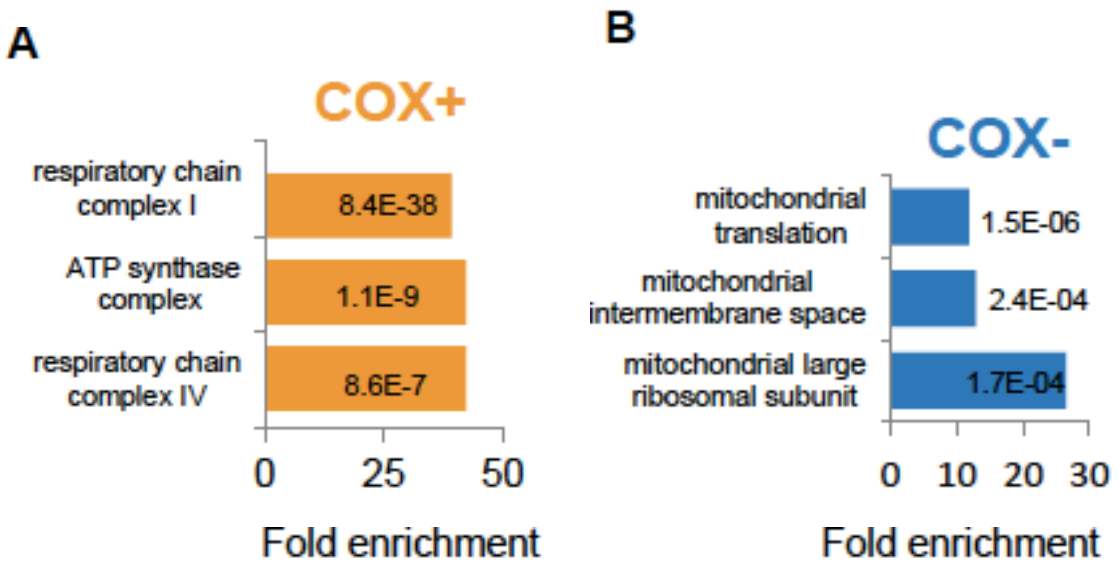

Figure 4.4.2: Annotations of mitochondrial proteins with increased expression in COX+ and COX- muscle fiber pools. A: COX+ fibers, B: COX- fibers.

We performed an unsupervised hierarchical cluster analysis of the mitochondrial proteins with significantly different expression between COX+ and COX- fibers (**Figure 4.4.3**). These mitochondrial proteins were present in at least 2 of the 3 patients and filled any missing values by data imputation. In contrast to COX+ fibers, in COX- fibers, there were 29 up-regulated mitochondrial proteins, including STOML2, PHB2 and OPA1 involved in cristae remodeling, mitochondrial fusion and respiratory supercomplex assembly, as well as the mitochondrial chaperones TRAP1 and HSD1. In COX+ fibers, 82 proteins were up-regulated and related to oxidative phosphorylation and electron transport. These results suggest COX- fibers may compensate for the defective bioenergetic supply through up-regulating some key proteins in the process of mitochondrial network organization.

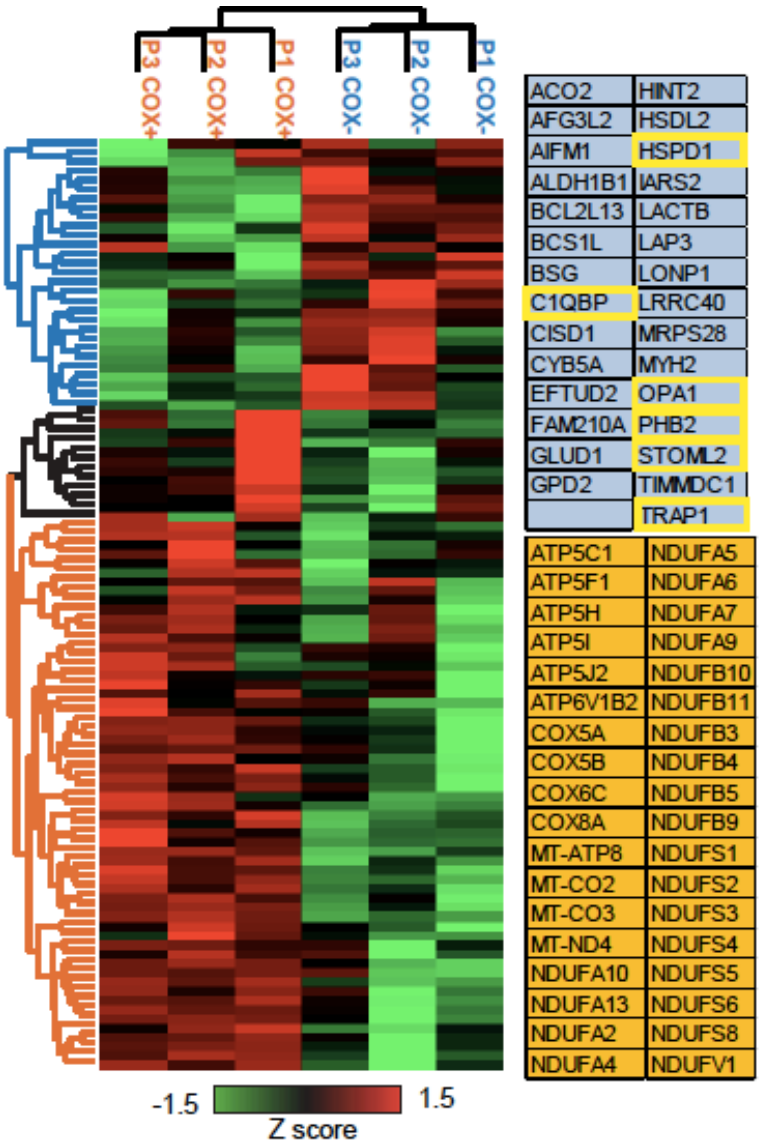

Figure 4.4.3: Hierarchical cluster analysis of the mitochondrial proteins with significantly different expression between COX+ and COX- fibers. The differences in expression of two clusters clearly separated the two main branches of the dendrogram, consisting of COX+ (orange) and COX- (blue) fibers.

4.5 Comparison of the mitochondrial proteome of individual CPEO patients

Our LCM-based quantitative proteomic approach can elucidate the proteome bias caused by mitochondrial disease of each patient, implement analyses of mitochondrial proteomics in individual CPEO patients, and compare protein expression between COX+ and COX- fibers individually. In each patient, PCA showed a clear separation between COX+ and COX- fiber pools (in triplicates) along component one, which defines the largest difference in the dataset

(**Figure 4.5.1A**). In all CPEO patients, the separation was driven by a highly significant enrichment in components of the respiratory chain in COX+ fibers ($p<10^{-9}$) while the drivers of the separation in COX- fibers were markedly heterogeneous (**Figure 4.5.1B**). These proteins could have some implication for potential clinical inference, since they may be involved in protective compensation reactions to mitochondria dysfunction in the specific patients.

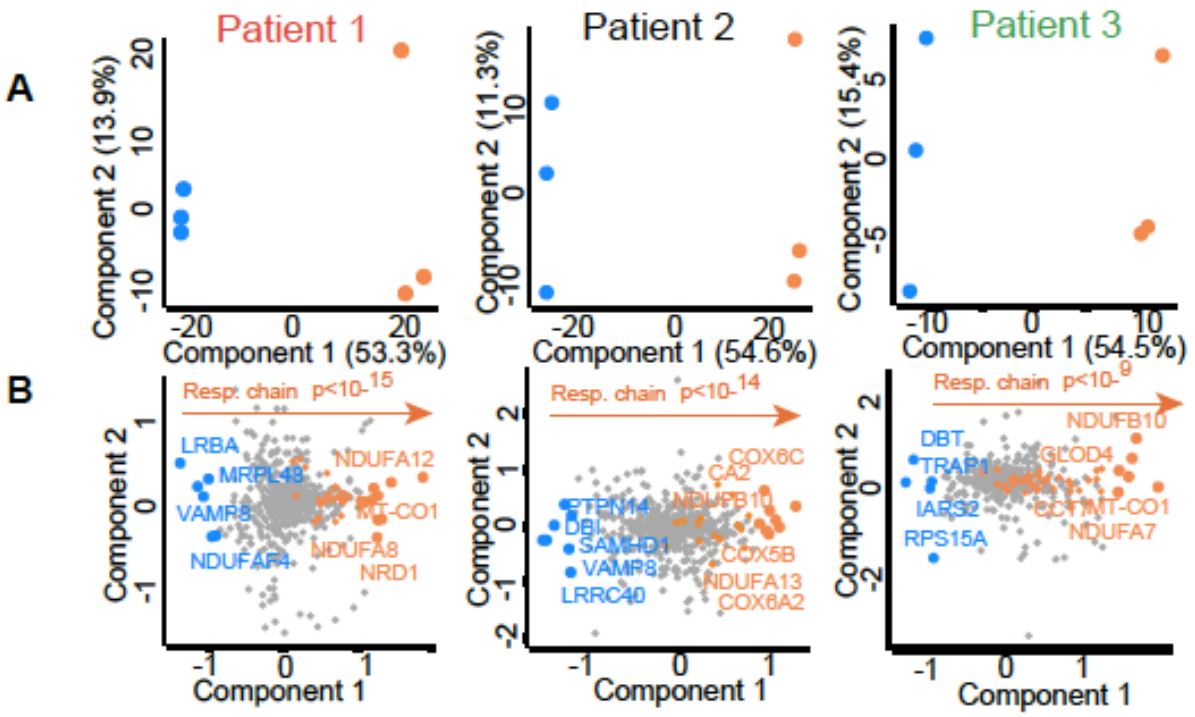

Figure 4.5.1: Patient-specific protein expression of mitochondrial diseases. A. Separation by PCA of COX+ (orange) and COX- (blue) fiber pools of each patient. B. Corresponding loadings driving the separation, with annotation enrichments and p values indicated by arrows.

Furthermore, we performed for each patient a T-test comparing COX+ and COX- fiber pools to highlight the significant differences in their mitochondrial proteome. 11 proteins with significantly higher expression in COX+ fibers were common to all three patients and over 50-fold upregulated in annotations pertaining to the respiratory chain and electron transport. However, only one protein, component 1 Q subcomponent-binding protein (C1QBP/p32), was commonly upregulated in COX- fibers of all three patients, which is a ubiquitously expressed

protein localized predominantly in the mitochondrial matrix and with poorly characterized function.

4.6 Mitochondrial protein analysis at the single fiber level

Regional specificity is enabled to microscopically isolate defined cell types with specific biological information by the means of LCM approach, which conduces to obtain deeper proteome coverage. With the help of COX/SDH double-labeling histochemistry as a morphological reference, we excised 20 serial sections of individual muscle fibers (COX+ and COX-) from 10 µm cross-sections of muscle biopsies for each patient (**Figure 4.2.1**). With this procedure, each single fiber encompasses 400 µm of tissue. We isolated three COX+ and three COX- single fibers from each patient. The serial sections of the same fiber were pooled and processed together for single-shot MS analysis. Previous studies have suggested that MS-based proteomics allows to directly quantify different myosin isoforms and thus determine fiber type [101].

Skeletal muscles are heterogeneous tissues and classified in different fiber types based on their expression of myosin heavy chain (MHC) isoforms. Human slow-type 1 fibers contain a higher oxidative metabolism and more mitochondria than the fast-type 2A and 2X fibers, which are characterized by a higher expression of glycolytic enzymes [101]. Hence, we next focused on the mitochondrial proteome of pure slow-type 1 fibers, analyzing the expression of mitochondrial proteins that were expressed in at least 9 of 12 slow fibers (217 proteins). We could separate COX+ and COX- slow fibers along component 2, which was driven by the significantly different expression of respiratory chain components (**Figure 4.6.1**). Here, several mitochondrial proteins were found with higher levels of expression in COX- slow fibers, which had the key control effect on the architecture of the inner mitochondrial membrane.

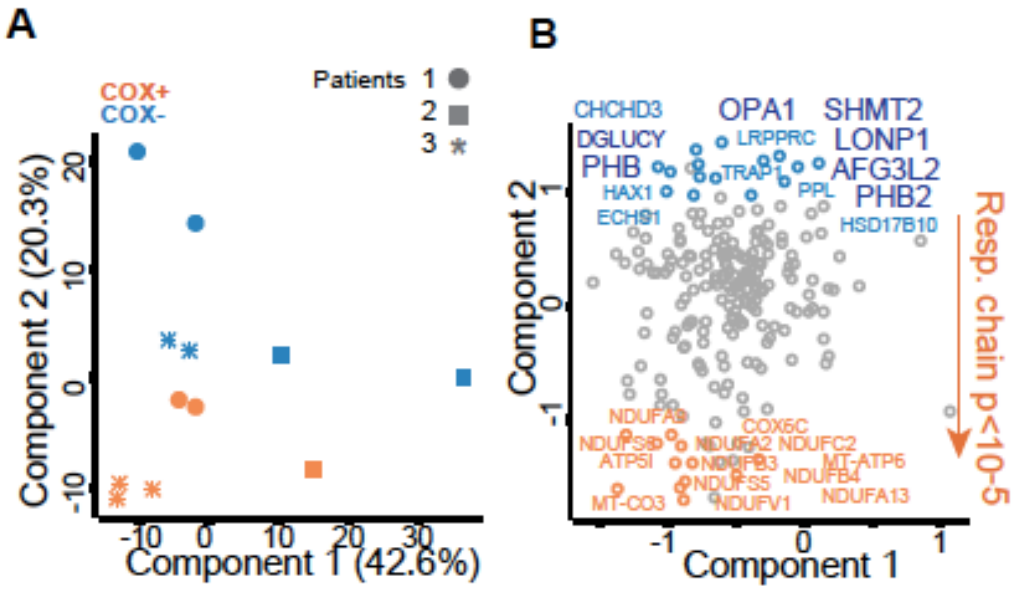

Figure 4.6.1: Mitochondrial proteins expression in single slow-type muscle fiber. A: PCA of mitochondrial proteins in pure slow single fibers. The fibers from three patients segregate into COX+ (orange) and COX- (blue) along component two. (b) Corresponding loadings with significant enrichments indicated by the arrow.

Comparing the abundance of these proteins in single COX+ and COX- slow-type 1 fibers, we found several proteins displayed a significantly higher expression in COX-slow-type 1 fibers (**Figure 4.6.2**). One of those proteins is the Dynamin-related GTPase OPA1, a key member of the mitochondrial contact site and cristae organizing system (MICOS) involved in cristae remodeling and fusion [115]. ATPase family gene 3-like 2 (AFG3L2) and Lon peptidase (LONP1) also present a significant overexpression in COX- slow-type 1 fibers. The former is a catalytic subunit of mitochondrial AAA protease, which degrades misfolded proteins, controls mitochondrial fragmentation and calcium dynamics [116, 117]. The latter is a master regulator of mitochondrial protein homeostasis, which is reported to regulate the important mtDNA structure factor, mitochondrial transcription factor A (TFAM). Two prohibitin family members, prohibitin 1 (PHB1) and PHB2, which are scaffolding proteins of the inner mitochondrial membrane and regulate the cell proliferation and cristae morphogenesis[118], were also significantly upregulated in COX- compared to COX+ slow fibers. And the mitochondrial folate enzyme serine hydroxy-methyl transferase 2 (SHMT2) was also with a higher expression, which controls the expression of respiratory chain enzymes [119].

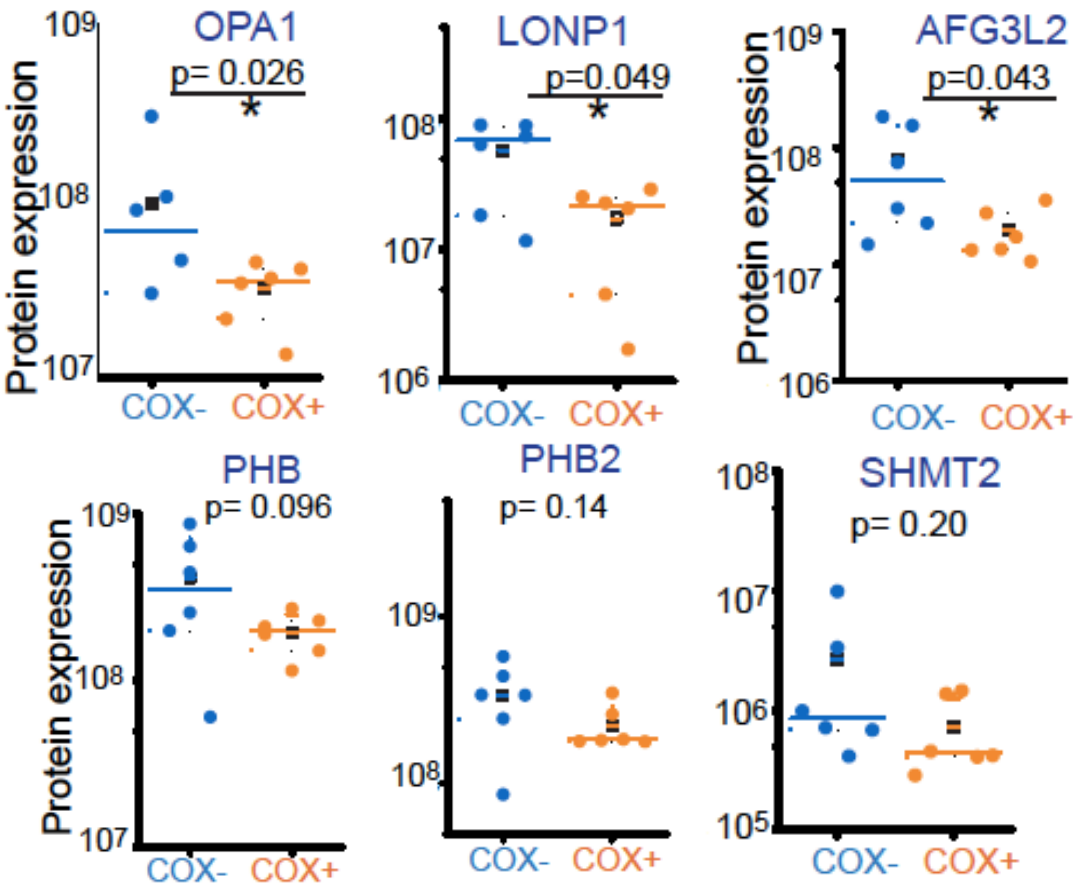

Figue 4.6.2: Comparison of mitochondrial proteins expression between COX- (blue) and COX+ (orange) slow-type fibers. The individual data point (each one fiber) are superimposed to the box plot showing the median, 25th and 75th percentile. Whiskers show standard deviation. The barred square shows the mean.

5. Discussion

Mitochondrial disorders are multisystem diseases characterized by defects in the assembly and function of the mitochondrial respiratory chain. They often affect the structure and function of tissues or organs with higher energy demands resulting in defective oxidative phosphorylation (OXPHOS). Skeletal muscle is a frequent target tissue in mitochondrial disorders. More than 250 pathogenic mtDNA mutations have been reported currently, and the heteroplasmy level of them will decide the expression of disease-associated proteins and the severity of mitochondrial disorders. Patient muscles therefore acquire a heterogeneous composition of compensated COX+ and noncompensated COX- fibers, which can serve as a diagnostic signpost of mitochondrial disease.

Mass spectrometry (MS)-based proteomics are typically used to provide identification and quantification of diverse proteins on the level of whole tissues or organs, but this also produces an averaging effect causing interference with the deeper biological analysis. Hence, it is becoming widely recognized that it is of advantage for the understanding of the tissue-specific pathogenesis of individual diseases to isolate specific spatially defined regions or cell types of samples, thus contributing to the recognition of candidate biomarkers or potential therapeutic targets at molecular level. Laser capture microdissection (LCM) is an easy and practical approach to capture morphologically defined cell types preserving abundant biological information. In our study, we performed LCM of 10 μm sections of muscle fibers and combined it with a sensitive quantitative proteomic workflow featuring recent technological advances. Since skeletal muscles are composed of variable fractions of slow and fast fibers which have different contractile properties, mitochondrial content and general metabolic features, our approach focuses on the complete proteomic analysis at the level of single muscle fiber via LCM.

5.1 The workflow with laser capture microdissection and proteomic analysis

Our study shows the feasibility of using skeletal muscle cells of COX+ and COX- fibers isolated by LCM for MS-based proteome analysis at both individual level and single fiber level. The summarized strategy is outlined in Figure 4.1. Here, we performed the approach of LCM to isolate serial sections of COX+ and COX- cells based on COX/SDH staining and collected these pure cells to make proteomic analyses that allowed the discovery of mitochondrial molecular properties and unknown disease-associated signal pathways. It was confirmed that LCM-based enrichment is ideal for the proteomic analysis[120, 121].

However, it is challenging to execute the analysis of quantitative proteomics via peptide labeling strategies because of minute amounts of samples yielded. Our LCM-based proteomic approach combines single-shot measurements of patient samples with a fixed resource consisting of extensively fractionated peptide libraries using label free quantification (MaxLFQ), which increases peptide and protein identification and can be queried with a broad spectrum of molecular and diagnostic questions. Our LCM-based workflow allowed the quantification of over 4000 proteins from <50ng of patient material in just 3 hours of measurement time, despite the dynamic range of the muscle fiber proteome driven by highly abundant sarcomeric proteins. This depth allowed us to conduct a detailed analysis of the muscle proteome, providing refined quantification of all respiratory complexes and almost complete coverage of the TCA cycle and mitochondrial translation.

5.2. Advantages and Limitations of LCM

The advantages of LCM are intuitively clear including speed, practicability, precision as well as versatility. We can excise thousands of interesting cells per cap in a short time frame through adjusting the proper laser spot size, microdissection speed and precision [122]. Structures of both the targeted regions and the residual tissues can remain intact and avoid the waste of samples. Therefore, various cell types can be isolated sequentially from the same tissue cross-section by LCM. The LCM approach can be applied to different cell or tissue

preparations, even those archival sections [123]. Furthermore, LCM can spatially define the interesting cells or regions via the traditional H&E or immunohistochemistry staining. In the end, the analysis of DNA, RNA and proteins will not be affected due to the protection of film and the use of low power laser. Banks et al. reported that profiles of proteins collected by LCM were close to those collected by conventional methods [124].

There are only few limitations of LCM. Since coverslip can prevent films adhering interesting cells from dropping to the cap of tubes, all slides prepared to operate microdissection do not allow cover glasses on the surface of tissue sections. That is the main limitation of LCM. Due to the absence of a coverslip, there is a lower optical resolution in the slide that affect the precision of microdissection in the capture of specific cells from complex tissues without typically morphological characters. Section staining is an effective measurement to address it. Another limitation only occurring occasionally is failure to remove captured cells from the slide to the cap. That is typically caused by loss of cellular adherence to the PEN membrane which results from the lower laser energy or deficient dehydration of tissues. In spite of these limitations, LCM remains an ideal tool to rapidly collect a large number of interesting cells or tissue regions from heterogeneous tissues.

5.3 The different proteome level between COX+ and COX- fibers

In muscle, COX+ and COX- fibers coexist and show a mosaic distribution in patients with mtDNA-associated mitochondrial disease. Our results clearly show that COX+ and COX- fibers are significantly different at the proteome level. Despite expressing respiratory chain components at a significantly lower level than COX+ fibers, COX- fibers upregulate mitochondrial ribosome proteins and proteins involved in the control of translation. This change is likely a compensatory mechanism, since the upregulation of mitochondrial translation is associated with partial rescue of respiration [125]. COX- fibers also increase the expression of several mitochondrial chaperones and of stomatin-like protein 2 (STOML2), which organizes cardiolipin-enriched microdomains in the inner mitochondrial membrane and controls the assembly of functional respiratory supercomplexes [126]. Among the proteins

upregulated in COX- fibers, only the complement component 1 Q subcomponent-binding protein (C1QBP) was common to all patients analyzed. Mutations in C1QBP have recently been detected in a patient with mitochondrial cardiomyopathy [127] and furthermore, C1QBP-knockout (KO) mice show respiratory-chain deficiencies due to impaired mitochondrial protein synthesis [128]. While being in line with previous reports in cellular models of mitochondrial disease, our proteomic data now quantify the molecular changes induced by mtDNA mutation at the level of the direct targets of disease, the muscle fibers.

Moreover, a number of mitochondrial proteins associated with mitochondrial quality control and mitochondrial dynamics were upregulated in COX- fibers. As discussed, mitochondrial quality control pathways are fundamental to numerous neurodegenerative diseases [129]. The pathogenesis of MELAS and LHON caused by mtDNA mutations for example, have been demonstrated to involve dysfunctions of mitochondrial protein quality control system [129-131]. The enhancement of mitochondrial quality control is best perceived as a three-tiered mechanism to maintain the functionality of mitochondria [129]. The first line of defense involves chaperones, proteases and ubiquitin-proteasome system to sustain mitochondrial protein homeostasis at the molecular level. ATP-dependent protease Lon for example, a mitochondrial matrix protein, has been demonstrated to recognize and degrade various abnormal and damaged polypeptides [132]. Meanwhile, molecular chaperone proteins of the mitochondrial matrix, the Hsp60, Hsp70 and Hsp100 family, can stabilize misfolded proteins or mediate protein dissolution against aggregation [133]. The second mechanism is concerned with mitochondrial morphology and dynamic fission and fusion events to compensate for damaged mitochondria at the organelle level. The third mechanism focuses on clearance of damaged mitochondria and cells through mitophagy and apoptosis at the cellular level. In relation to the second mechanism, we found the dynamin-like GTPase OPA1 is significantly upregulated in COX- fibers. The dynamin-like GTPase OPA1 mediates mitochondrial fusion, ensuring cristae morphogenesis and the maintenance of mtDNA, and protection against apoptosis [134]. The overexpression of OPA1 is therefore likely to serve as an early response to maintain functional stabilization of mitochondrial network by preventing fragmentation of mitochondria [135].

5.4 Proteomic analysis based on the level of individual muscle fiber

The approach of laser capture microdissection (LCM), a powerful technique to precisely harvest the pure cell populations or cell regions targeted by morphology from heterogenous tissue sections and proteomics, can investigate the proteomic responses to mitochondrial dysfunction intra-individually, eliminating confounding bias. Additionally, since the clinical biopsies of patients with mitochondrial disease are routinely small in size and quantity, it is necessary to take full advantage of the limited tissues and cells available. Therefore, comparisons were made between COX+ and COX- cells not only on the whole samples but also on the single patient and single fiber type level in our study. Muscle fiber type abnormalities, including the distribution and size of type I and II fibers, have been reported in various mitochondrial diseases. In patients with adult mitochondrial myopathy, skeletal muscle fiber type transformation from type I to type II is described [136] and likewise, in a rat model of mitochondrial myopathy [137]. In contrast, type I fiber predominance has been demonstrated in children with mitochondrial myopathy. This predominance may serve as a compensatory mechanism for mitochondrial electron transport chain abnormalities as there is higher abundance of mitochondria in type I fibers compared to type II fibers, therefore they are able to partially enhance the energy production in damaged cells. The underlying pathogenesis of these changes in muscle fiber types however are poorly understood.

The main feature of our LCM-based proteomic approach is the ability to analyze mitochondrial disease in individual muscle fibers, by following and cutting the same fiber across 20 serial muscle sections. In this pathological context, the heterogeneous composition of skeletal muscle into slow-type 1 and fast-type 2 fibers, which have different mitochondrial content, is superimposed onto the pathological process giving rise to the COX+ and COX- fiber mosaic. To reduce the variables causing this extreme heterogeneity we selected a pool of single muscle fibers defined as type-1 slow, based on the expression of MYH7, the slow myosin heavy chain isoform. With this approach we eliminated confounding effects of the heterogeneous muscle fiber type composition, revealing a coordinated increase of the OPA1-dependent cristae remodeling program in the mitochondria of COX- slow fibers. This

pathway controls the tightening of the mitochondrial cristae, which results in higher respiratory efficiency and limits the production of reactive oxygen species and cytochrome c release [138]. This fiber type-specific analysis also revealed that mitochondrial folate enzyme, serine hydroxyl-methyl transferase 2 (SHMT2), as specifically upregulated in COX- fibers. It has recently been shown that defects in this enzyme cause impaired expression of respiratory chain components by interfering with tRNA methylation and causing ribosome stalling [119].

5.5 Potential mechanisms of mitochondrial diseases

Our data indicate that mitochondrial diseases are associated with complex proteomic rearrangements of the mitochondrial cristae affecting respiratory supercomplex formation and bioenergetic efficiency. Furthermore, our analysis also points to increased mitochondrial translation in COX- fibers. It remains to be determined whether the combination of the observed compensatory mechanisms ultimately provides rescue from the energy imbalance caused by respiratory chain defects, or whether it contributes to the pathogenesis of the disease by causing proteotoxic stress and inducing the mitochondrial unfolded protein response. Mechanistic studies of how defects in the assembly and function of the respiratory chain are communicated to the cell nucleus is necessary to understand the complex progressive pathogenesis of mitochondrial disease and to provide a molecular basis for targeted interventions.

5.6 The prospect of clinical applications

Precision medicine is defined as an approach to disease treatment and prevention that seeks to maximize effectiveness by considering individual variability in genes, environment, and lifestyle. Since mitochondrial diseases are highly heterogeneous in genetics, biochemistry and phenotype, this strategy has significant potential for their diagnosis and treatment. The high accuracy and sensitivity of mass spectrometry-based proteomics is well suitable to integrate proteomics into the developmental framework of precision medicine [139], and may help to bridge the gap between genotype and phenotype of diseases. The utilization of proteomic

technologies has resulted in great progress in precision medicine by facilitating detection of protein biomarkers, proteomics-based molecular diagnostics, as well as protein biochips and pharmacoproteomics [139]. Clinical proteomic-driven precision medicine has been reported in a range of diseases, such as in cancer, respiratory diseases, multiple sclerosis and diabetes [140-142]. However, applications in mitochondrial diseases have not been reported so far.

Our group has established a fixed resource containing deep human skeletal muscle proteomes and built a streamlined LCM-based proteomics workflow applied to muscle biopsies and single muscle fibers. This will hopefully contribute to the development of precision medicine in mitochondrial diseases and provide novel insights in disease mechanisms, signaling pathways and sensitive biomarkers for molecular diagnosis and therapeutic monitoring. In conclusion, these findings have the potential to offer holistic insights into the molecular status of one individual, facilitate rapid and detailed diagnosis, as well as personalized prevention and therapy strategies.

6. Summary

Mitochondrial disorders are multisystem diseases characterized by defects in the assembly and function of the mitochondrial respiratory chain, which usually attack skeletal muscles resulting in the mosaicism of COX+ and COX- fibers. Laser capture microdissection (LCM) is an effective tool to harvest specific cell types from heterogeneous tissues on the basis of histochemical staining. Combining LCM and mass spectrometry in the study of mitochondrial disorders opens the way for identification and analysis of proteins from specific cell or tissue types at the individual level.

We designed an LCM-based proteomic workflow which can extract large amounts of biological information from minute amounts of frozen muscle biopsies, laser-microdissected muscle fiber sections and isolated single fibers in a short time. We utilized LCM to isolate COX+ and COX- cells from muscle biopsies of chronic progressive external ophthalmoplegia (CPEO) patients based on the combined cytochrome oxidase/succinate dehydrogenase (COX/SDH) staining, followed by their proteomic analysis at both the individual level and the single fiber level. Comparing these two muscle fiber types, we found COX+ and COX- fibers to be significantly different at the proteome level. COX- fibers upregulate the expression of mitochondrial ribosome proteins and proteins involved in the control of translation, which would be a compensatory mechanism in mitochondrial disorder. Moreover, the expression of optic atrophy protein 1 (OPA1) is likely to serve as an early response to maintain functional stabilization of the mitochondrial network. Moreover, we observed single fiber type-specific information showing that increased expression of fatty acid oxidation enzymes occurs in slow muscle fibers.

Our study reveals compensatory mechanisms of skeletal muscle fibers for the energy deficit caused by mitochondrial dysfunction and suggests novel pathogenetic mechanisms in CPEO patients. The combination of LCM and quantitative proteomics may help to bridge the gap

between genotype and phenotype and to tackle unsolved questions in mitochondrial precision medicine.

Zusammenfassung

Mitochondriale Erkrankungen sind multisystemische Syndrome, die durch Defekte in der Zusammensetzung und Funktion der mitochondrialen Atmungskette gekennzeichnet sind. Sie betreffen häufig die Skelettmuskulatur und führen dort zu einem Mosaik aus Cytochrom c-Oxidase-positiven (COX+) und –negativen (COX-) Fasern. Die Laser-Capture-Mikrodissektion (LCM) ist ein effektives Werkzeug, um bestimmte Zelltypen aus heterogenen Geweben auf Basis einer histochemischen Färbung zu gewinnen. Die Kombination von LCM und Massenspektrometrie in der Erforschung von mitochondrialen Störungen eröffnet den Weg für die Identifizierung und Analyse von Proteinen bestimmter Zell- oder Gewebearten auf individueller Ebene.

Wir haben einen LCM-basierten proteomischen Workflow entwickelt, der große Mengen an biologischer Information aus winzigen Mengen an gefrorenen Muskelbiopsien, laser-mikrodissektierten Muskelfaserabschnitten und isolierten Einzelfasern in kurzer Zeit extrahieren kann. Wir haben LCM verwendet, um COX+ und COX- Zellen aus Muskelbiopsien von Patienten mit chronisch progressiver externer Ophthalmoplegie (CPEO) zu isolieren, basierend auf der kombinierten Färbung von Cytochromoxidase/Succinatdehydrogenase (COX/SDH), gefolgt von ihrer proteomischen Analyse sowohl auf individueller als auch auf Einzelfaserebene. Im Vergleich dieser beiden Muskelfasertypen haben wir festgestellt, dass COX+ und COX- Fasern auf Proteomniveau signifikant unterschiedlich sind. COX- Fasern hochregulieren die Expression von mitochondrialen Ribosomenproteinen und Proteinen, die an der Kontrolle der Translation beteiligt sind, was einen Kompensationsmechanismus bei mitochondrialen Störungen darstellt. Darüber hinaus ist die vermehrte Expression des Optic Atrophy-Proteins 1 (OPA1) wahrscheinlich eine frühe Regulation zur Aufrechterhaltung eines stabilen mitochondrialen Netzwerks. Darüber hinaus konnten wir eine erhöhte Expression von Fettsäureoxidations-Enzymen in Typ 2-Muskelfasern beobachten.

Unsere Studie zeigt kompensatorische Mechanismen von Skelettmuskelfasern für das durch mitochondriale Dysfunktion verursachte Energiedefizit und ergibt Hinweise für neue pathogenetische Mechanismen. Die Kombination von LCM und quantitativer Proteomik kann dazu beitragen, die Lücke zwischen Genotyp und Phänotyp zu schließen und offene Fragen in der mitochondrialen Präzisionsmedizin zu beantworten.

7. Attachment

7.1 Bibliography

1. Colombini, M., *Mitochondrial outer membrane channels.* Chem Rev, 2012. **112**(12): p. 6373-87.
2. Herst, P.M., et al., *Functional Mitochondria in Health and Disease.* Front Endocrinol (Lausanne), 2017. **8**: p. 296.
3. Cavalier-Smith, T., *The origin of nuclei and of eukaryotic cells.* Nature, 1975. **256**: p. 463.
4. Gray, M.W., *Mitochondrial evolution.* Cold Spring Harb Perspect Biol, 2012. **4**(9): p. a011403.
5. Kurland, C.G. and S.G. Andersson, *Origin and evolution of the mitochondrial proteome.* Microbiol Mol Biol Rev, 2000. **64**(4): p. 786-820.
6. Palmer, J.D., *Organelle genomes: going, going, gone!* Science, 1997. **275**(5301): p. 790-1.
7. Papa, S., et al., *Coupling mechanisms in anionic substrate transport across the inner membrane of rat-liver mitochondria.* J Bioenerg, 1971. **1**(3): p. 287-307.
8. Papa, S., et al., *The oxidative phosphorylation system in mammalian mitochondria.* Adv Exp Med Biol, 2012. **942**: p. 3-37.
9. Volobueva, A.S., et al., *Mitochondrial genome variability: the effect on cellular functional activity.* Ther Clin Risk Manag, 2018. **14**: p. 237-245.
10. Bonn, F., et al., *Functional evaluation of paraplegin mutations by a yeast complementation assay.* Hum Mutat, 2010. **31**(5): p. 617-21.
11. Nass, S. and M.M. Nass, *INTRAMITOCHONDRIAL FIBERS WITH DNA CHARACTERISTICS. II. ENZYMATIC AND OTHER HYDROLYTIC TREATMENTS.* J Cell Biol, 1963. **19**: p. 613-29.
12. Anderson, S., et al., *Sequence and organization of the human mitochondrial genome.* Nature, 1981. **290**(5806): p. 457-65.
13. Moraes, C.T., *What regulates mitochondrial DNA copy number in animal cells?* Trends Genet, 2001. **17**(4): p. 199-205.
14. Wiesner, R.J., J.C. Ruegg, and I. Morano, *Counting target molecules by exponential polymerase chain reaction: copy number of mitochondrial DNA in rat tissues.* Biochem Biophys Res Commun, 1992. **183**(2): p. 553-9.
15. Kasamatsu, H. and J. Vinograd, *Replication of circular DNA in eukaryotic cells.* Annu Rev Biochem, 1974. **43**(0): p. 695-719.
16. Fernandez-Silva, P., J.A. Enriquez, and J. Montoya, *Replication and transcription of mammalian mitochondrial DNA.* Exp Physiol, 2003. **88**(1): p. 41-56.
17. Attardi, G. and G. Schatz, *Biogenesis of mitochondria.* Annu Rev Cell Biol, 1988. **4**: p. 289-333.
18. Shadel, G.S. and D.A. Clayton, *Mitochondrial DNA maintenance in vertebrates.* Annu Rev Biochem, 1997. **66**: p. 409-35.
19. Schwartz, M. and J. Vissing, *Paternal inheritance of mitochondrial DNA.* N Engl J Med, 2002. **347**(8): p. 576-80.
20. Zhao, X., et al., *Paternal inheritance of mitochondrial DNA in the sheep (Ovine aries).* Sci China C Life Sci, 2001. **44**(3): p. 321-6.
21. Balsa, E., et al., *NDUFA4 is a subunit of complex IV of the mammalian electron transport chain.* Cell Metab, 2012. **16**(3): p. 378-86.

22. You, K.R., et al., *Cytochrome c oxidase subunit III: a molecular marker for N-(4-hydroxyphenyl)retinamise-induced oxidative stress in hepatoma cells.* J Biol Chem, 2002. **277**(6): p. 3870-7.
23. Rotig, A., *Human diseases with impaired mitochondrial protein synthesis.* Biochim Biophys Acta, 2011. **1807**(9): p. 1198-205.
24. Reinecke, F., J.A. Smeitink, and F.H. van der Westhuizen, *OXPHOS gene expression and control in mitochondrial disorders.* Biochim Biophys Acta, 2009. **1792**(12): p. 1113-21.
25. Zhang, J., et al., *ROS and ROS-Mediated Cellular Signaling.* Oxid Med Cell Longev, 2016. **2016**: p. 4350965.
26. Scarpulla, R.C., R.B. Vega, and D.P. Kelly, *Transcriptional integration of mitochondrial biogenesis.* Trends Endocrinol Metab, 2012. **23**(9): p. 459-66.
27. Cunningham, J.T., et al., *mTOR controls mitochondrial oxidative function through a YY1-PGC-1alpha transcriptional complex.* Nature, 2007. **450**(7170): p. 736-40.
28. Brown, W.M., M. George, Jr., and A.C. Wilson, *Rapid evolution of animal mitochondrial DNA.* Proc Natl Acad Sci U S A, 1979. **76**(4): p. 1967-71.
29. Holt, I.J., A.E. Harding, and J.A. Morgan-Hughes, *Deletions of muscle mitochondrial DNA in patients with mitochondrial myopathies.* Nature, 1988. **331**(6158): p. 717-9.
30. Wallace, D.C., et al., *Mitochondrial DNA mutation associated with Leber's hereditary optic neuropathy.* Science, 1988. **242**(4884): p. 1427-30.
31. Chinnery, P.F. and E.A. Schon, *Mitochondria.* J Neurol Neurosurg Psychiatry, 2003. **74**(9): p. 1188-99.
32. Larsson, N.G. and D.A. Clayton, *Molecular genetic aspects of human mitochondrial disorders.* Annu Rev Genet, 1995. **29**: p. 151-78.
33. Wang, J., et al., *An integrated approach for classifying mitochondrial DNA variants: one clinical diagnostic laboratory's experience.* Genet Med, 2012. **14**(6): p. 620-6.
34. Luft, R., et al., *A case of severe hypermetabolism of nonthyroid origin with a defect in the maintenance of mitochondrial respiratory control: a correlated clinical, biochemical, and morphological study.* J Clin Invest, 1962. **41**: p. 1776-804.
35. Gorman, G.S., et al., *Prevalence of nuclear and mitochondrial DNA mutations related to adult mitochondrial disease.* Ann Neurol, 2015. **77**(5): p. 753-9.
36. Spinazzola, A. and M. Zeviani, *Mitochondrial diseases: a cross-talk between mitochondrial and nuclear genomes.* Adv Exp Med Biol, 2009. **652**: p. 69-84.
37. Lightowlers, R.N., R.W. Taylor, and D.M. Turnbull, *Mutations causing mitochondrial disease: What is new and what challenges remain?* Science, 2015. **349**(6255): p. 1494-9.
38. Thorburn, D.R. and H.H. Dahl, *Mitochondrial disorders: genetics, counseling, prenatal diagnosis and reproductive options.* Am J Med Genet, 2001. **106**(1): p. 102-14.
39. Chinnery, P.F., *Mitochondrial Disorders Overview*, in *GeneReviews((R))*, M.P. Adam, et al., Editors. 1993, University of Washington, Seattle University of Washington, Seattle. GeneReviews is a registered trademark of the University of Washington, Seattle. All rights reserved.: Seattle (WA).
40. Taylor, R.W. and D.M. Turnbull, *Mitochondrial DNA mutations in human disease.* Nat Rev Genet, 2005. **6**(5): p. 389-402.
41. Cao, Z., et al., *Mitochondrial DNA deletion mutations are concomitant with ragged red regions of individual, aged muscle fibers: analysis by laser-capture microdissection.* Nucleic Acids Res, 2001. **29**(21): p. 4502-8.
42. Brown, D.T., et al., *Random genetic drift determines the level of mutant mtDNA in human primary oocytes.* Am J Hum Genet, 2001. **68**(2): p. 533-6.
43. Hauswirth, W.W. and P.J. Laipis, *Mitochondrial DNA polymorphism in a maternal lineage of Holstein cows.* Proc Natl Acad Sci U S A, 1982. **79**(15): p. 4686-90.

44. Chinnery, P.F., et al., *The inheritance of mitochondrial DNA heteroplasmy: random drift, selection or both?* Trends Genet, 2000. **16**(11): p. 500-5.
45. Chinnery, P.F. and D.C. Samuels, *Relaxed replication of mtDNA: A model with implications for the expression of disease.* Am J Hum Genet, 1999. **64**(4): p. 1158-65.
46. Orsucci, D., G. Siciliano, and M. Mancuso, *Revealing the Complexity of Mitochondrial DNA-Related Disorders.* EBioMedicine, 2018. **30**: p. 3-4.
47. van der Bliek, A.M., Q. Shen, and S. Kawajiri, *Mechanisms of mitochondrial fission and fusion.* Cold Spring Harb Perspect Biol, 2013. **5**(6).
48. Twig, G., et al., *Fission and selective fusion govern mitochondrial segregation and elimination by autophagy.* Embo j, 2008. **27**(2): p. 433-46.
49. de Brito, O.M. and L. Scorrano, *Mitofusin 2 tethers endoplasmic reticulum to mitochondria.* Nature, 2008. **456**(7222): p. 605-10.
50. Hayashi, G. and G. Cortopassi, *Oxidative stress in inherited mitochondrial diseases.* Free Radic Biol Med, 2015. **88**(Pt A): p. 10-7.
51. Zhang, J., et al., *A novel ADOA-associated OPA1 mutation alters the mitochondrial function, membrane potential, ROS production and apoptosis.* Sci Rep, 2017. **7**(1): p. 5704.
52. Olichon, A., et al., *Loss of OPA1 perturbates the mitochondrial inner membrane structure and integrity, leading to cytochrome c release and apoptosis.* J Biol Chem, 2003. **278**(10): p. 7743-6.
53. Elachouri, G., et al., *OPA1 links human mitochondrial genome maintenance to mtDNA replication and distribution.* Genome Res, 2011. **21**(1): p. 12-20.
54. Amati-Bonneau, P., et al., *OPA1 mutations induce mitochondrial DNA instability and optic atrophy 'plus' phenotypes.* Brain, 2008. **131**(Pt 2): p. 338-51.
55. Hudson, G., et al., *Mutation of OPA1 causes dominant optic atrophy with external ophthalmoplegia, ataxia, deafness and multiple mitochondrial DNA deletions: a novel disorder of mtDNA maintenance.* Brain, 2008. **131**(Pt 2): p. 329-37.
56. Rouzier, C., et al., *The MFN2 gene is responsible for mitochondrial DNA instability and optic atrophy 'plus' phenotype.* Brain, 2012. **135**(Pt 1): p. 23-34.
57. Westermann, B., *Mitochondrial fusion and fission in cell life and death.* Nat Rev Mol Cell Biol, 2010. **11**(12): p. 872-84.
58. Merz, S. and B. Westermann, *Genome-wide deletion mutant analysis reveals genes required for respiratory growth, mitochondrial genome maintenance and mitochondrial protein synthesis in Saccharomyces cerevisiae.* Genome Biol, 2009. **10**(9): p. R95.
59. Suzuki, M., et al., *The solution structure of human mitochondria fission protein Fis1 reveals a novel TPR-like helix bundle.* J Mol Biol, 2003. **334**(3): p. 445-58.
60. Brooks, C., et al., *Bak regulates mitochondrial morphology and pathology during apoptosis by interacting with mitofusins.* Proc Natl Acad Sci U S A, 2007. **104**(28): p. 11649-54.
61. Suen, D.F., K.L. Norris, and R.J. Youle, *Mitochondrial dynamics and apoptosis.* Genes Dev, 2008. **22**(12): p. 1577-90.
62. Waterham, H.R., et al., *A lethal defect of mitochondrial and peroxisomal fission.* N Engl J Med, 2007. **356**(17): p. 1736-41.
63. Nakamura, T. and S.A. Lipton, *Redox modulation by S-nitrosylation contributes to protein misfolding, mitochondrial dynamics, and neuronal synaptic damage in neurodegenerative diseases.* Cell Death Differ, 2011. **18**(9): p. 1478-86.
64. Franchi, L., R. Munoz-Planillo, and G. Nunez, *Sensing and reacting to microbes through the inflammasomes.* Nat Immunol, 2012. **13**(4): p. 325-32.
65. Shimada, K., et al., *Oxidized mitochondrial DNA activates the NLRP3 inflammasome during apoptosis.* Immunity, 2012. **36**(3): p. 401-14.

66. Gross, O., et al., *The inflammasome: an integrated view.* Immunol Rev, 2011. **243**(1): p. 136-51.
67. Horng, T., *Calcium signaling and mitochondrial destabilization in the triggering of the NLRP3 inflammasome.* Trends Immunol, 2014. **35**(6): p. 253-61.
68. Nunnari, J. and A. Suomalainen, *Mitochondria: in sickness and in health.* Cell, 2012. **148**(6): p. 1145-59.
69. Koopman, W.J., P.H. Willems, and J.A. Smeitink, *Monogenic mitochondrial disorders.* N Engl J Med, 2012. **366**(12): p. 1132-41.
70. Cho, D.H., T. Nakamura, and S.A. Lipton, *Mitochondrial dynamics in cell death and neurodegeneration.* Cell Mol Life Sci, 2010. **67**(20): p. 3435-47.
71. Pickles, S., P. Vigie, and R.J. Youle, *Mitophagy and Quality Control Mechanisms in Mitochondrial Maintenance.* Curr Biol, 2018. **28**(4): p. R170-r185.
72. Bohovych, I., S.S. Chan, and O. Khalimonchuk, *Mitochondrial protein quality control: the mechanisms guarding mitochondrial health.* Antioxid Redox Signal, 2015. **22**(12): p. 977-94.
73. Palmer, C.S., et al., *The regulation of mitochondrial morphology: intricate mechanisms and dynamic machinery.* Cell Signal, 2011. **23**(10): p. 1534-45.
74. Stotland, A. and R.A. Gottlieb, *Mitochondrial quality control: Easy come, easy go.* Biochim Biophys Acta, 2015. **1853**(10 Pt B): p. 2802-11.
75. Shintani, T. and D.J. Klionsky, *Autophagy in health and disease: a double-edged sword.* Science, 2004. **306**(5698): p. 990-5.
76. Okamoto, K., *Mitochondria breathe for autophagy.* Embo j, 2011. **30**(11): p. 2095-6.
77. Nakahira, K., et al., *Autophagy proteins regulate innate immune responses by inhibiting the release of mitochondrial DNA mediated by the NALP3 inflammasome.* Nat Immunol, 2011. **12**(3): p. 222-30.
78. Rabilloud, T., et al., *Two-dimensional electrophoresis of human placental mitochondria and protein identification by mass spectrometry: toward a human mitochondrial proteome.* Electrophoresis, 1998. **19**(6): p. 1006-14.
79. Verma, M., et al., *Proteomic analysis of cancer-cell mitochondria.* Nat Rev Cancer, 2003. **3**(10): p. 789-95.
80. Cherry, C., et al., *2016: A 'Mitochondria' Odyssey.* Trends Mol Med, 2016. **22**(5): p. 391-403.
81. Raimundo, N., *Mitochondrial pathology: stress signals from the energy factory.* Trends Mol Med, 2014. **20**(5): p. 282-92.
82. Tocchi, A., et al., *Mitochondrial dysfunction in cardiac aging.* Biochim Biophys Acta, 2015. **1847**(11): p. 1424-33.
83. Payne, B.A. and P.F. Chinnery, *Mitochondrial dysfunction in aging: Much progress but many unresolved questions.* Biochim Biophys Acta, 2015. **1847**(11): p. 1347-53.
84. Sun, N., R.J. Youle, and T. Finkel, *The Mitochondrial Basis of Aging.* Mol Cell, 2016. **61**(5): p. 654-666.
85. Gygi, S.P., et al., *Evaluation of two-dimensional gel electrophoresis-based proteome analysis technology.* Proc Natl Acad Sci U S A, 2000. **97**(17): p. 9390-5.
86. Braun, R.J., et al., *Two-dimensional electrophoresis of membrane proteins.* Anal Bioanal Chem, 2007. **389**(4): p. 1033-45.
87. Gygi, S.P., et al., *Quantitative analysis of complex protein mixtures using isotope-coded affinity tags.* Nat Biotechnol, 1999. **17**(10): p. 994-9.
88. Ong, S.E., et al., *Stable isotope labeling by amino acids in cell culture, SILAC, as a simple and accurate approach to expression proteomics.* Mol Cell Proteomics, 2002. **1**(5): p. 376-86.
89. Ross, P.L., et al., *Multiplexed protein quantitation in Saccharomyces cerevisiae using amine-reactive isobaric tagging reagents.* Mol Cell Proteomics, 2004. **3**(12): p. 1154-69.

90. Miyagi, M. and K.C. Rao, *Proteolytic 18O-labeling strategies for quantitative proteomics.* Mass Spectrom Rev, 2007. **26**(1): p. 121-36.
91. Aebersold, R. and M. Mann, *Mass-spectrometric exploration of proteome structure and function.* Nature, 2016. **537**(7620): p. 347-55.
92. Taylor, R.W., et al., *The diagnosis of mitochondrial muscle disease.* Neuromuscul Disord, 2004. **14**(4): p. 237-45.
93. Deshmukh, A.S., et al., *Deep proteomics of mouse skeletal muscle enables quantitation of protein isoforms, metabolic pathways, and transcription factors.* Mol Cell Proteomics, 2015. **14**(4): p. 841-53.
94. Thakur, D., et al., *Microproteomic analysis of 10,000 laser captured microdissected breast tumor cells using short-range sodium dodecyl sulfate-polyacrylamide gel electrophoresis and porous layer open tubular liquid chromatography tandem mass spectrometry.* J Chromatogr A, 2011. **1218**(45): p. 8168-74.
95. Gozal, Y.M., et al., *Merger of laser capture microdissection and mass spectrometry: a window into the amyloid plaque proteome.* Methods Enzymol, 2006. **412**: p. 77-93.
96. Park, S.K., et al., *A quantitative analysis software tool for mass spectrometry-based proteomics.* Nat Methods, 2008. **5**(4): p. 319-22.
97. Cox, J. and M. Mann, *MaxQuant enables high peptide identification rates, individualized p.p.b.-range mass accuracies and proteome-wide protein quantification.* Nat Biotechnol, 2008. **26**(12): p. 1367-72.
98. Rabilloud, T., et al., *Comparative proteomics as a new tool for exploring human mitochondrial tRNA disorders.* Biochemistry, 2002. **41**(1): p. 144-50.
99. Tryoen-Toth, P., et al., *Proteomic consequences of a human mitochondrial tRNA mutation beyond the frame of mitochondrial translation.* J Biol Chem, 2003. **278**(27): p. 24314-23.
100. Edhager, A.V., et al., *Proteomic investigation of cultivated fibroblasts from patients with mitochondrial short-chain acyl-CoA dehydrogenase deficiency.* Mol Genet Metab, 2014. **111**(3): p. 360-368.
101. Murgia, M., et al., *Single Muscle Fiber Proteomics Reveals Fiber-Type-Specific Features of Human Muscle Aging.* Cell Rep, 2017. **19**(11): p. 2396-2409.
102. Old, S.L. and M.A. Johnson, *Methods of microphotometric assay of succinate dehydrogenase and cytochrome c oxidase activities for use on human skeletal muscle.* Histochem J, 1989. **21**(9-10): p. 545-55.
103. Emmert-Buck, M.R., et al., *Laser capture microdissection.* Science, 1996. **274**(5289): p. 998-1001.
104. Koob, A.O., et al., *Protein analysis through Western blot of cells excised individually from human brain and muscle tissue.* Anal Biochem, 2012. **425**(2): p. 120-4.
105. Kulak, N.A., et al., *Minimal, encapsulated proteomic-sample processing applied to copy-number estimation in eukaryotic cells.* Nat Methods, 2014. **11**(3): p. 319-24.
106. Kulak, N.A., P.E. Geyer, and M. Mann, *Loss-less Nano-fractionator for High Sensitivity, High Coverage Proteomics.* Mol Cell Proteomics, 2017. **16**(4): p. 694-705.
107. Cox, J., et al., *Andromeda: a peptide search engine integrated into the MaxQuant environment.* J Proteome Res, 2011. **10**(4): p. 1794-805.
108. Tyanova, S., et al., *The Perseus computational platform for comprehensive analysis of (prote)omics data.* Nat Methods, 2016. **13**(9): p. 731-40.
109. Cox, J., et al., *Accurate proteome-wide label-free quantification by delayed normalization and maximal peptide ratio extraction, termed MaxLFQ.* Mol Cell Proteomics, 2014. **13**(9): p. 2513-26.

110. Scheltema, R.A., et al., *The Q Exactive HF, a Benchtop mass spectrometer with a pre-filter, high-performance quadrupole and an ultra-high-field Orbitrap analyzer.* Mol Cell Proteomics, 2014. **13**(12): p. 3698-708.
111. Tyanova, S., T. Temu, and J. Cox, *The MaxQuant computational platform for mass spectrometry-based shotgun proteomics.* Nat Protoc, 2016. **11**(12): p. 2301-2319.
112. Espina, V., et al., *Laser-capture microdissection.* Nat Protoc, 2006. **1**(2): p. 586-603.
113. Greaves, L.C., et al., *Mitochondrial DNA defects and selective extraocular muscle involvement in CPEO.* Invest Ophthalmol Vis Sci, 2010. **51**(7): p. 3340-6.
114. Cram, L.S., M. Lalande, and B.H. Mayall, *In memoriam: Samuel A. Latt (1938-1988).* Cytometry, 1989. **10**(1): p. 1-2.
115. Kozjak-Pavlovic, V., *The MICOS complex of human mitochondria.* Cell Tissue Res, 2017. **367**(1): p. 83-93.
116. Konig, T., et al., *The m-AAA Protease Associated with Neurodegeneration Limits MCU Activity in Mitochondria.* Mol Cell, 2016. **64**(1): p. 148-162.
117. Koppen, M., et al., *Variable and tissue-specific subunit composition of mitochondrial m-AAA protease complexes linked to hereditary spastic paraplegia.* Mol Cell Biol, 2007. **27**(2): p. 758-67.
118. Merkwirth, C. and T. Langer, *Prohibitin function within mitochondria: essential roles for cell proliferation and cristae morphogenesis.* Biochim Biophys Acta, 2009. **1793**(1): p. 27-32.
119. Morscher, R.J., et al., *Mitochondrial translation requires folate-dependent tRNA methylation.* Nature, 2018. **554**(7690): p. 128-132.
120. Vogel, A., et al., *Mechanisms of Laser-Induced Dissection and Transport of Histologic Specimens.* Biophysical Journal, 2007. **93**(12): p. 4481-4500.
121. Umar, A., et al., *NanoLC-FT-ICR MS improves proteome coverage attainable for approximately 3000 laser-microdissected breast carcinoma cells.* Proteomics, 2007. **7**(2): p. 323-9.
122. Fend, F. and M. Raffeld, *Laser capture microdissection in pathology.* J Clin Pathol, 2000. **53**(9): p. 666-72.
123. Zanni, K.L. and G.K. Chan, *Laser capture microdissection: understanding the techniques and implications for molecular biology in nursing research through analysis of breast cancer tumor samples.* Biol Res Nurs, 2011. **13**(3): p. 297-305.
124. Banks, R.E., et al., *The potential use of laser capture microdissection to selectively obtain distinct populations of cells for proteomic analysis--preliminary findings.* Electrophoresis, 1999. **20**(4-5): p. 689-700.
125. Karicheva, O.Z., et al., *Correction of the consequences of mitochondrial 3243A>G mutation in the MT-TL1 gene causing the MELAS syndrome by tRNA import into mitochondria.* Nucleic Acids Res, 2011. **39**(18): p. 8173-86.
126. Mitsopoulos, P., et al., *Stomatin-like protein 2 is required for in vivo mitochondrial respiratory chain supercomplex formation and optimal cell function.* Mol Cell Biol, 2015. **35**(10): p. 1838-47.
127. Feichtinger, R.G., et al., *Biallelic C1QBP Mutations Cause Severe Neonatal-, Childhood-, or Later-Onset Cardiomyopathy Associated with Combined Respiratory-Chain Deficiencies.* Am J Hum Genet, 2017. **101**(4): p. 525-538.
128. Yagi, M., et al., *p32/gC1qR is indispensable for fetal development and mitochondrial translation: importance of its RNA-binding ability.* Nucleic Acids Res, 2012. **40**(19): p. 9717-37.
129. Baker, M.J., C.S. Palmer, and D. Stojanovski, *Mitochondrial protein quality control in health and disease.* Br J Pharmacol, 2014. **171**(8): p. 1870-89.

130. Felk, S., et al., *Activation of the mitochondrial protein quality control system and actin cytoskeletal alterations in cells harbouring the MELAS mitochondrial DNA mutation.* J Neurol Sci, 2010. **295**(1-2): p. 46-52.
131. Tun, A.W., et al., *Profiling the mitochondrial proteome of Leber's Hereditary Optic Neuropathy (LHON) in Thailand: down-regulation of bioenergetics and mitochondrial protein quality control pathways in fibroblasts with the 11778G>A mutation.* PLoS One, 2014. **9**(9): p. e106779.
132. Torregiani, F. and C. La Cavera, *[Differential diagnosis of acute abdomen and latrodectism].* Minerva Chir, 1990. **45**(5): p. 303-5.
133. Voos, W. and K. Rottgers, *Molecular chaperones as essential mediators of mitochondrial biogenesis.* Biochim Biophys Acta, 2002. **1592**(1): p. 51-62.
134. Landes, T., et al., *OPA1 (dys)functions.* Semin Cell Dev Biol, 2010. **21**(6): p. 593-8.
135. Duvezin-Caubet, S., et al., *Proteolytic processing of OPA1 links mitochondrial dysfunction to alterations in mitochondrial morphology.* J Biol Chem, 2006. **281**(49): p. 37972-9.
136. Gehrig, S.M., et al., *Altered skeletal muscle (mitochondrial) properties in patients with mitochondrial DNA single deletion myopathy.* Orphanet J Rare Dis, 2016. **11**(1): p. 105.
137. Wright, J.J., *Reticular activation and the dynamics of neuronal networks.* Biol Cybern, 1990. **62**(4): p. 289-98.
138. Varanita, T., et al., *The OPA1-dependent mitochondrial cristae remodeling pathway controls atrophic, apoptotic, and ischemic tissue damage.* Cell Metab, 2015. **21**(6): p. 834-44.
139. Duarte, T.T. and C.T. Spencer, *Personalized Proteomics: The Future of Precision Medicine.* Proteomes, 2016. **4**(4).
140. Zhou, L., et al., *Clinical proteomics-driven precision medicine for targeted cancer therapy: current overview and future perspectives.* Expert Rev Proteomics, 2016. **13**(4): p. 367-81.
141. Xu, W., et al., *Preoperative Chemotherapy for Gastric Cancer: Personal Interventions and Precision Medicine.* Biomed Res Int, 2016. **2016**: p. 3923585.
142. Teran, L.M., et al., *Respiratory proteomics: from descriptive studies to personalized medicine.* J Proteome Res, 2015. **14**(1): p. 38-50.

7.2 Abbreviations

ATP	Adenosine triphosphate
ADT	Adenosine diphosphate
ARE	Antioxidant responsive elements
ADOA	Autosomal dominant optic atrophy
AFG3L2	ATPase family gene 3-like 2
ASC	Apoptosis-associated speck-like adaptor protein
ACADS	Acyl-CoA Dehydrogenase Short Chain
AGC	Automatic gain control
16-BAC	16-benzyldimethyln-hexadecylammonium chloride
CoQ	Coenzyme Q
COX	Cytochrome oxidase
CO	Cytochrome oxidase
CPEO	Chronic progressive external ophthalmoplegia
CTAB	Cetyl trimethylammonium bromide
C1QBP	Component 1 Q subcomponent-binding protein
D-loop	Displacement loop
Drp1	Dynamin-related protein 1
2DE	Two-dimensional
ETC	Electron transport chain
ETF	Electron transfer flavoprotein
ER	Endoplasmic reticulum
ESI	Electrospray ionization
FABP5	Fatty acid binding protein 5
FAD	Flavin adenine dinucleotide

HSP60	Heat shock protein 60
HCD	Higher-energy collisional dissociation
IMM	Inner mitochondria membrane
IL-1β	Interleukin-1β
ICATs	Isotope-coded affinity tags
iTRAQ	Isobaric tags for relative and absolute quantitation
KSS	Kearns-Sayre syndrome
LHON	Leber hereditary optic neuropathy
LC-MS	Liquid chromatography coupled with MS
LCM	Laser capture microdissection
LONP1	Lon peptidase
mtDNA	Mitochondrial DNA
MELAS	Mitochondrial encephalomyopathy with lactic acidosis and stroke-like episodes
MERRF	Myoclonic epilepsy with ragged red fibers
Mfn1	Mitofusin 1
MS	Mass spectrometry
MICOS	Mitochondrial contact site and cristae organizing system
NRF-1	Nuclear respiratory factor-1
nDNA	Nuclear DNA
NLRP1	Nucleotide-binding domain and leucine-rich repeat containing proteins 1
NLR	NOD-like receptor
OMM	Outer mitochondria membrane
O_2	Oxygen
OXPHOS	Oxidative phosphorylation

OPA1	Optic atrophy protein 1
PHB1	Prohibitin 1
PLA2	Phospholipases A2
PTMs	Post-translational modifications
PCA	Principal component analysis
rRNA	Ribosomal RNA
ROS	Reactive oxygen species
SDH	Succinate dehydrogenase
SNO-Drp1	S-nitrosylated Drp1
SDS-PAGE	Sodium dodecyl sulphate-polyacrylamide gel electrophoresis
SILAC	Stable isotope labeling with amino acids
STOML2	Stomatin-like protein 2
SHMT2	Serine hydroxyl-methyl transferase 2
TCA	Tricarboxylic acid
TFAM	Transcription factor A
tRNA	Transfer RNA
TM	Tansmembrane domain
UPS	Ubiquitin–proteasome system
UPRmt	Mitochondrial unfolded protein response
VDAC	Voltage-dependent anion channel
wt	Wildtype

7.3 Acknowledgments

My deepest gratitude goes first and foremost to my supervisor, Prof. Dr. med Thomas Klopstock, for offering the opportunity to work on this project, as well as for his constant encouragement and intellectual guidance of my thesis. I have learned a lot about science in general and the mitochondrial disorders in particular during the past three years.

Secondly, I would like to express my special gratitude to Dr. Marta Murgia for her hard work with the proteomics analysis and for teaching me the proteomics techniques. Without her contribution this thesis would not have been possible. I also need thank Prof. Dr. Matthias Mann for his valuable suggestions for this thesis, thank Phd students Sophia Doll and Philipp Geyer for their technical support of proteomics and thank Phd students Sarah Stenton for her modification of the language expression.

Then, I would like to thank Dr. med. Christoph Laub for teaching me the operation of laser capture microdissection. I'm thankful for my lovely colleagues of Friedrich-Baur-Institute, Brandstetter Ira, Claudia Catarino, Büchner Boriana, for their friendly help in my study and life in Germany.

Finally, I want to express my deepest thankfulness to my families and my friends, especially my parents for their continuous support and encourage during all the years of my studies.

7.4 Eidesstattliche Versicherung

Eidesstattliche Versicherung

Jing Tan

Name, Vorname

Ich erkläre hiermit an Eides statt,

dass ich die vorliegende Dissertation mit dem Thema

Laser capture microdissection of single muscle fibers for mitochondrial proteomic investigations

selbständig verfasst, mich außer der angegebenen keiner weiteren Hilfsmittel bedient und alle Erkenntnisse, die aus dem Schrifttum ganz oder annähernd übernommen sind, als solche kenntlich gemacht und nach ihrer Herkunft unter Bezeichnung der Fundstelle einzeln nachgewiesen habe.

Ich erkläre des Weiteren, dass die hier vorgelegte Dissertation nicht in gleicher oder in ähnlicher Form bei einer anderen Stelle zur Erlangung eines akademischen Grades eingereicht wurde.

22.02.2019, Muenchen	Jing Tan
Ort, Datum	Unterschrift Doktorandin/Doktorand

7.5 Übereinstimmungserklärung

Erklärung zur Übereinstimmung der gebundenen Ausgabe der Dissertation mit der elektronischen Fassung

Jing Tan
Name, Vorname

Hiermit erkläre ich, dass die elektronische Version der eingereichten Dissertation mit dem Titel *Laser capture microdissection of single muscle fibers for mitochondrial proteomic investigations*

in Inhalt und Formatierung mit den gedruckten und gebundenen Exemplaren übereinstimmt.

22.02,2019, Muenchen	Jing Tan
Ort, Datum	Unterschrift Doktorandin/Doktorand